The Plant Cell, Vol. 32: 1102–1123, April 2020, www.plantcell.org © 2020 ASPB.

IbBBX24 Promotes the Jasmonic Acid Pathway and Enhances Fusarium Wilt Resistance in Sweet Potato

Huan Zhang,[a,b,1] Qian Zhang,[a,1] Hong Zhai,[a] Shaopei Gao,[a] Li Yang,[c] Zhen Wang,[a] Yuetong Xu,[d] Jinxi Huo,[a] Zhitong Ren,[a] Ning Zhao,[a] Xiangfeng Wang,[d] Jigang Li,[b] Qingchang Liu,[a,2] and Shaozhen He[a,2]

[a] Key Laboratory of Sweet Potato Biology and Biotechnology, Ministry of Agriculture and Rural Affairs/Beijing Key Laboratory of Crop Genetic Improvement/Laboratory of Crop Heterosis & Utilization and Joint Laboratory for International Cooperation in Crop Molecular Breeding, Ministry of Education, College of Agronomy & Biotechnology, China Agricultural University, Beijing 100193, China
[b] State Key Laboratory of Plant Physiology and Biochemistry, College of Biological Sciences, China Agricultural University, Beijing 100193, China
[c] State Key Laboratory of Protein and Plant Gene Research, The Peking-Tsinghua Center for Life Sciences, School of Advanced Agricultural Sciences and School of Life Sciences, Peking University, 100871 Beijing, China
[d] Department of Crop Genomics and Bioinformatics, College of Agronomy & Biotechnology, China Agricultural University, Beijing 100193, China

ORCID IDs: 0000-0002-6190-296X (H.Z.); 0000-0002-6631-2213 (Q.Z.); 0000-0001-9797-9961 (H.Z.); 0000-0003-1084-0516 (S.P.G.); 0000-0003-3842-6341 (L.Y.); 0000-0003-1182-6775 (Z.W.); 0000-0002-7936-0361 (Y.T.X.); 0000-0001-8032-7756 (J.X.H.); 0000-0001-9650-0584 (Z.T.R.); 0000-0002-2979-7602 (N.Z.); 0000-0002-6406-5597 (X.F.W.); 0000-0002-4395-2656 (J.G.L.); 0000-0002-9127-3885 (Q.C.L.); 0000-0003-0212-5803 (S.H.H.)

Cultivated sweet potato (*Ipomoea batatas*) is an important source of food for both humans and domesticated animals. Here, we show that the B-box (BBX) family transcription factor IbBBX24 regulates the jasmonic acid (JA) pathway in sweet potato. When *IbBBX24* was overexpressed in sweet potato, JA accumulation increased, whereas silencing this gene decreased JA levels. RNA sequencing analysis revealed that IbBBX24 modulates the expression of genes involved in the JA pathway. IbBBX24 regulates JA responses by antagonizing the JA signaling repressor IbJAZ10, which relieves IbJAZ10's repression of IbMYC2, a JA signaling activator. IbBBX24 binds to the *IbJAZ10* promoter and activates its transcription, whereas it represses the transcription of *IbMYC2*. The interaction between IbBBX24 and IbJAZ10 interferes with IbJAZ10's repression of IbMYC2, thereby promoting the transcriptional activity of IbMYC2. Overexpressing *IbBBX24* significantly increased Fusarium wilt disease resistance, suggesting that JA responses play a crucial role in regulating Fusarium wilt resistance in sweet potato. Finally, overexpressing *IbBBX24* led to increased yields in sweet potato. Together, our findings indicate that IbBBX24 plays a pivotal role in regulating JA biosynthesis and signaling and increasing Fusarium wilt resistance and yield in sweet potato, thus providing a candidate gene for developing elite crop varieties with enhanced pathogen resistance but without yield penalty.

INTRODUCTION

Sweet potato (*Ipomoea batatas*) is an economically important root and tuber crop that is widely used as an industrial and bioenergy resource worldwide. Fusarium wilt, a disease caused by *Fusarium oxysporum* f. sp *batatas* (*Fob*), leads to yield losses of 10% to 50% in sweet potato (Ogawa and Komada, 1985; Li et al., 2017). The hemibiotrophic fungus *F. oxysporum* causes vascular wilt disease in over 100 plant species and significantly limits the production of many crops, such as tomato (*Solanum lycopersicum*), tobacco (*Nicotiana tabacum*), and cotton (*Gossypium spp*; Michielse and Rep, 2009; Cole et al., 2014). The symptoms of vascular wilt disease include vascular browning, stunting, and progressive wilting, eventually leading to plant death (Michielse and Rep, 2009).

Jasmonic acid (JA) was initially identified as a stress-related hormone in plants. JA and its methyl ester (MeJA) and isoleucine conjugate (JA-Ile) are derivatives of a class of fatty acids that are collectively known as jasmonates (JAs; Campos et al., 2014). JA plays an essential role in plant defense responses against necrotrophic and hemibiotrophic pathogens, especially fungi. Mutants of JA biosynthetic and signaling genes display increased susceptibility to various fungi. For example, the Arabidopsis (*Arabidopsis thaliana*) JA biosynthesis mutant *fad3 fad7 fad8* is significantly more susceptible to *Pythium mastophorum* than is the wild type (McConn et al., 1997; Stintzi et al., 2001), while a mutation in *JAI1*, the tomato homolog of the Arabidopsis jasmonate receptor gene *CORONATINE INSENSITIVE1* (*COI1*), results in increased susceptibility to *Botrytis cinerea* and *F. oxysporum* (Li et al., 2004; Thaler et al., 2004; Abuqamar et al., 2008). Conversely, the Arabidopsis mutant *cev1*, in which JA is constitutively produced and the JA-related downstream genes *PLANT DEFENSIN1.2* (*PDF1.2*) and *THIONIN2.1* are constitutively expressed, exhibits enhanced defense responses against fungal pathogens (Ellis and Turner, 2001).

[1] These authors contributed equally to this work.
[2] Address correspondence to sunnynba@cau.edu.cn and liuqc@cau.edu.cn.
The authors responsible for the distribution of materials integral to the findings presented in this article in accordance with the policy described in the Instructions for Authors (www.plantcell.org) are Shaozhen He (sunnynba@cau.edu.cn) and Qingchang Liu (liuqc@cau.edu.cn).
www.plantcell.org/cgi/doi/10.1105/tpc.19.00641

IN A NUTSHELL

Background: Sweet potato is an economically important root and tuber crop that is widely used as an industrial and bioenergy resource worldwide and as an important source of food for both humans and domesticated animals. However, the quality and production of sweet potato are severely threatened by Fusarium wilt disease caused by a hemibiotrophic fungus (abbreviated as *Fob*), which causes vascular dysfunction in over 100 plant species. Jasmonic acid (JA), a stress-related hormone in plants, plays an essential role in plant defense responses against pathogens. Various transcription factors are involved in regulating JA-responsive gene expression. B-box (BBX) proteins mediate transcriptional regulation and protein–protein interactions during multiple plant growth and developmental processes. However, whether BBX proteins function in plant defense responses remains unclear.

Question: Are BBX proteins involved in regulating Fusarium wilt resistance in sweet potato? If so, what are the underlying mechanisms?

Findings: The BBX-family transcription factor IbBBX24 regulates the JA pathway in sweet potato. When *IbBBX24* was overexpressed in sweet potato, JA accumulation increased, whereas silencing this gene decreased JA levels. Overexpressing *IbBBX24* significantly increased Fusarium wilt resistance, suggesting that JA responses play a crucial role in regulating Fusarium wilt resistance in sweet potato. RNA-sequencing analysis revealed that IbBBX24 modulates the expression of genes involved in the JA pathway. Furthermore, we determined that IbBBX24 modulates the JA pathway via two mechanisms. First, IbBBX24 represses the expression of *IbJAZ10*, encoding a JA signaling repressor, but activates the expression of *IbMYC2*, encoding a JA signaling activator, by binding directly to their promoters. Second, IbBBX24 physically interacts with IbJAZ10, thus releasing IbMYC2 from the IbJAZ10 repressor. Overexpressing *IbBBX24* also led to increased yield in sweet potato, suggesting that *IbBBX24* may serve as an ideal candidate gene for developing elite crop varieties with enhanced pathogen resistance but without yield penalty.

Next steps: In future research, the mechanisms underlying *Fob* infection and IbBBX24-regulated JA biosynthesis and storage root yield in sweet potato need to be investigated. Moreover, the utilization of *IbBBX24* for enhancing disease resistance and yield in sweet potato could be an important task for geneticists and breeders.

The exogenous application of MeJA induces plant resistance to various pathogens (Sun et al., 2013; Król et al., 2015; Oliveira et al., 2015). JA responses are critical for resistance or susceptibility to *F. oxysporum*, depending on the pathogenesis mechanism, as demonstrated in plants such as Arabidopsis and tomato (Epple et al., 1997; Berrocal-Lobo and Molina, 2004; Thaler et al., 2004; McGrath et al., 2005; Van Hemelrijck et al., 2006; Kidd et al., 2009; Thatcher et al., 2009; Cole et al., 2014). In transgenic plants overexpressing Arabidopsis *ETHYLENE RESPONSE FACTOR1*, Arabidopsis *ETHYLENE RESPONSE FACTOR2*, or *THIONIN2.1*, which display increased resistance to *F. oxysporum*, JA-responsive genes such as *PDF1.2* and *BASIC CHITINASE* are significantly activated (Epple et al., 1997; Berrocal-Lobo and Molina, 2004; McGrath et al., 2005). By contrast, the *esa1* mutant, with enhanced susceptibility to *F. oxysporum*, shows delayed induction of *PDF1.2* (Van Hemelrijck et al., 2006). Notably, the perturbation of JA signaling has no detectable effect on the susceptibility of tomato to *F. oxysporum* f. sp *lycopersici* (*Fol*; Cole et al., 2014; Di et al., 2017). However, although plants employ the JA-mediated pathway to defend against various microbial pathogens, some pathogens—including biotrophic and hemibiotrophic pathogens—produce and inject toxins and virulence effector proteins into host cells, thus evading the plant defense system by hijacking the JA-signaling pathway (Jiang et al., 2013; Cole et al., 2014; Gimenez-Ibanez et al., 2014; Yan and Xie, 2015).

The core JA-signaling module consists of the JA receptor COI1, a subset of jasmonate–ZIM domain (JAZ) repressor proteins, and the various transcription factors involved in regulating the expression of JA-responsive genes (Turner et al., 2002; Zhai et al., 2017). COI1, an F-box protein, interacts with multiple proteins to form the SCF^{COI1} E3 ubiquitin ligase complex (Xie et al., 1998; Devoto et al., 2002; Xu et al., 2002). JAZ proteins, which function as transcriptional repressors, contain an N-terminal domain, a central ZIM domain, and a C-terminal JA-associated (Jas) domain (Pauwels and Goossens, 2011; Zhai et al., 2017). These domains are responsible for the interactions of these proteins with different signaling partners. For example, the ZIM domain mediates the interaction of JAZ proteins with NOVEL INTERACTOR OF JAZ (Pauwels et al., 2010), and the Jas domain is responsible for interacting with COI1 and several families of transcription factors, including the bHLH transcription factors MYC2 to MYC4 and the R2R3-MYB transcription factors MYB21 and MYB24 (Chini et al., 2007; Pauwels and Goossens, 2011; Qi et al., 2011, 2015; Goossens et al., 2015). Crystal structure analysis demonstrated that COI1 and JAZ form a co-receptor complex with the bioactive form of JA, JA-Ile, indicating that JAZ proteins function as jasmonate co-receptors (Sheard et al., 2010; Zhai et al., 2017; Ruan et al., 2019). In the absence of JA-Ile, JAZ proteins act as repressors of the above-mentioned transcription factors; however, the presence of JA-Ile promotes the interaction between COI1 and JAZ proteins (Thines et al., 2007; Katsir et al., 2008; Melotto et al., 2008; Ruan et al., 2019), and the JAZ proteins are subsequently ubiquitinated by SCF^{COI1} and degraded through the 26S proteasome pathway (Thines et al., 2007; Melotto et al., 2008; Pauwels and Goossens, 2011; Zhai et al., 2017). Thus, the repression of the transcription factors is relieved, allowing them to activate the expression of JA-responsive genes (Pauwels and Goossens, 2011; Qi et al., 2011, 2015; Song et al., 2011; Zhai et al., 2015; Zhang et al., 2015). Among these transcription factors, MYC2 plays a key role in JA signaling (Boter et al., 2004; Lorenzo et al., 2004; Gfeller et al., 2010; Du et al., 2017; Ogawa et al., 2017; Zhai et al., 2017).

The B-box (BBX) proteins are a family of zinc-finger transcription factors that contain one or two B-box domains in their N termini and sometimes contain a CCT domain in their C termini (Gangappa and Botto, 2014). B-box motifs are involved in mediating transcriptional regulation and protein–protein interactions during multiple plant growth and developmental processes, including seedling photomorphogenesis (Datta et al., 2006, 2008; Jiang et al., 2012; Xu et al., 2016), photoperiodic regulation of flowering (Valverde et al., 2004; Kim et al., 2008; Hassidim et al., 2009; Ping et al., 2019), shade avoidance (Crocco et al., 2010; Wang et al., 2013a), pigment accumulation (Bai et al., 2019; Xiong et al., 2019), abiotic stress responses (Nagaoka and Takano, 2003; Liu et al., 2012; Crocco and Botto, 2013; Wang et al., 2013b; Crocco et al. 2018), and the signaling pathways of phytohormones such as gibberellins (GAs) and brassinosteroids (Weller et al., 2009; Luo et al., 2010; Fan et al., 2012; Yang et al., 2014). However, whether BBX proteins function in plant defense responses remains unclear.

In this study, we demonstrated that the BBX family transcription factor IbBBX24 participates in the JA pathway by modulating the JAZ-MYC module in sweet potato. In addition to regulating JA levels, IbBBX24 represses the expression of *IbJAZ10* but activates the expression of *IbMYC2* by directly binding to their promoters. Furthermore, IbBBX24 physically interacts with IbJAZ10, thus relieving its inhibition of IbMYC2 activity. Finally, the overexpression of *IbBBX24* led to increased *Fob* resistance and sweet potato yields. Collectively, our data demonstrate that IbBBX24 promotes the JA pathway and enhances Fusarium wilt resistance in sweet potato without yield penalty, providing insights into the roles of BBX transcription factors in regulating biotic stress resistance in plants.

RESULTS

IbBBX24 Is Highly Induced by *Fob* and MeJA

We previously demonstrated that JA signaling-related genes were upregulated in the *Fob*-resistant sweet potato line ND98 and that JA accumulated in ND98 after infection with *Fob* (Zhang et al., 2017a, 2017b). Here, we performed cDNA-amplified fragment length polymorphism (cDNA-AFLP) analysis to identify differentially expressed genes (DEGs) between ND98 and the *Fob*-susceptible variety Lizixiang after *Fob* infection. This analysis led to the identification of 32 genes whose expression was differentially regulated in ND98 and Lizixiang after *Fob* infection (Supplemental Table 1). Among these genes, four transcription factor genes, including *IbBBX24*, were differentially expressed in these *Fob*-susceptible and -resistant sweet potato plants. We also performed RNA-sequencing (RNA-seq) analysis to compare the transcriptomes of ND98 and Lizixiang. Notably, *IbBBX24* was significantly differentially expressed in these transcriptomes (Zhang et al., 2017b). Therefore, we focused on *IbBBX24* due to its potential role in *Fob* resistance in sweet potato.

We performed RT-qPCR to confirm the differential expression of *IbBBX24* in ND98 and Lizixiang. The expression of *IbBBX24* was induced almost 16-fold in ND98 but only 3-fold in Lizixiang at 1 d after *Fob* infection (Figure 1A). In addition, *IbBBX24* was induced 31-fold in ND98 and 3-fold in Lizixiang after 0.5 h of MeJA treatment (Figure 1B). In ND98, *IbBBX24* was expressed at the highest level in the roots of 4-week–old, in vitro–grown plants (Supplemental Figure 1A), whereas in 3-month–old field-grown plants, the highest expression level of *IbBBX24* was observed in leaves (Supplemental Figure 1B). Collectively, our data demonstrate that *IbBBX24* is highly induced by *Fob* and MeJA treatment in sweet potato and that it is expressed at significantly higher levels in ND98 than in Lizixiang.

Rapid amplification of cDNA ends assays revealed that the 1,069-bp full-length *IbBBX24* cDNA contains a 696-bp open reading frame (ORF). IbBBX24, belonging to clade IV of the BBX transcription factor family (Khanna et al., 2009), contains two conserved B-box domains and a VP motif (Figure 1C; Supplemental Figure 1C) and shares the closest phylogenetic relationship with AtBBX24 among Arabidopsis homologs (Figure 1C; Supplemental Figure 1C). The genomic sequence of *IbBBX24* contains three exons and two introns, which is similar to the exon–intron pattern of *AtBBX24* (Figure 1D). We examined the subcellular localization of IbBBX24 by transiently expressing the IbBBX24-GFP fusion protein in *Nicotiana benthamiana* epidermal cells. Confocal microscopy indicated that IbBBX24-GFP was located in the nucleus, whereas GFP alone was located throughout the cytosol (Supplemental Figure 1D).

We generated anti-IbBBX24 polyclonal antibodies; the specificity of the antibodies is demonstrated in Supplemental Figure 2. We used these antibodies to examine endogenous IbBBX24 protein levels in *Fob*-resistant line ND98 after *Fob* and MeJA treatment via immunoblot analysis. IbBBX24 protein levels increased in these plants in response to both *Fob* and MeJA treatment, peaking at 1 d after *Fob* infection and after 1 h of MeJA treatment (Figure 1E).

IbBBX24 Plays a Positive Role in Resistance to *Fob*

To further investigate whether *IbBBX24* contributes to *Fob* resistance in sweet potato, we generated 20 overexpression lines (designated as OE-1 to OE-20) and six RNA interference (RNAi) lines (designated as Ri-1 to Ri-6) from 1,500 and 1,200 cell aggregates, respectively, of the *Fob*-susceptible variety Lizixiang via *Agrobacterium tumefaciens*-mediated transformation (Supplemental Figure 3). After examining the levels of *IbBBX24* mRNA in these transgenic lines, we selected two overexpression lines (OE-3 and OE-16) and two RNAi lines (Ri-1 and Ri-3) for further study (Supplemental Figure 3J). To exclude the potential for cross silencing in the RNAi transgenic lines, we examined the expression levels of *IbBBX14*, *IbBBX21*, *IbBBX25*, and *IbBBX22* in two independent *IbBBX24-Ri* lines via RT-qPCR using sequence-specific primers (Supplemental Data Set 1). The encoded proteins of these four *BBX* genes showed highest homology to IbBBX24 (Supplemental Figure 4A). Only *IbBBX24* was downregulated in both *IbBBX24-Ri* lines, while the expression of *IbBBX14*, *IbBBX21*, *IbBBX25*, and *IbBBX22* either increased (*IbBBX14* and *IbBBX22*) or remained unchanged (*IbBBX21* and *IbBBX25*; Supplemental Figure 4B). These data suggest that these *IbBBX24*-homologous genes were not knocked down due to cross-silencing via RNAi.

The overexpression or loss-of-function of *AtBBX24* led to various physiological, developmental, and hormonal phenotypes in Arabidopsis (Li et al., 2014). However, the overexpression or

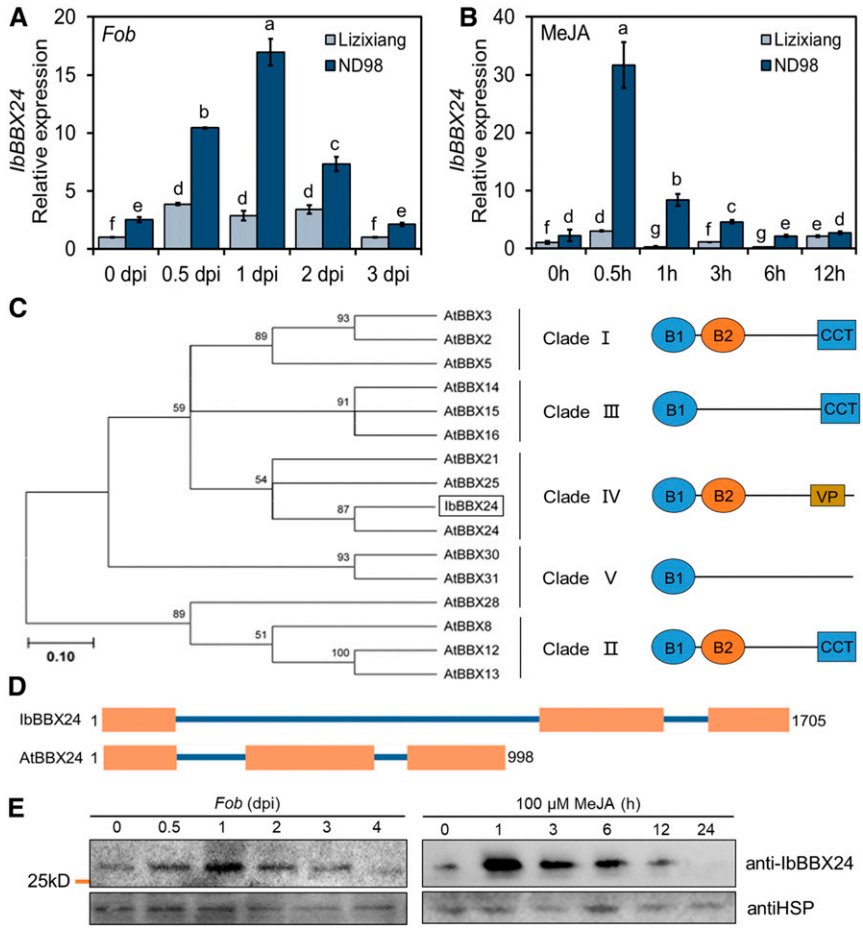

Figure 1. The Responses of *IbBBX24* to *Fob* and MeJA Treatment.

(A) Expression of *IbBBX24* in *Fob*-susceptible Lizixiang and *Fob*-resistant ND98 sweet potato after infection with *Fob*. The leaves of pot-grown Lizixiang and ND98 plants were sampled 0, 0.5, 1, 2, and 3 d after inoculation with *Fob* spores at a density of 1.5×10^7 mL^{-1}. The values were determined by RT-qPCR from three biological replicates consisting of pools of five plants. The error bars indicate ±SD ($n = 3$). Different lowercase letters indicate a significant difference at $P < 0.05$ based on Student's *t* test.

(B) Expression of *IbBBX24* in *Fob*-susceptible Lizixiang and *Fob*-resistant ND98 under 100 μM of MeJA treatment. Four-week–old in vitro-grown plants were submerged in half strength MS medium containing 100 μM of MeJA and sampled at 0, 0.5, 1, 3, 6, and 12 h after treatment. The error bars indicate ±SD ($n = 3$). The values were determined by RT-qPCR from three biological replicates consisting of pools of five plants.

(C) Phylogenetic analysis of BBX proteins from sweet potato (IbBBX24) and Arabidopsis using the neighbor-joining method in MEGA6.0 with 1,000 bootstrap iterations. The numbers at the nodes of the tree indicate bootstrap values from 1,000 replicates. IbBBX24 is marked with a black box.

(D) Comparison of the genomic structures of *IbBBX24* and *AtBBX24*. Boxes indicate exons, and lines indicate introns.

(E) Immunoblots showing that *Fob* and MeJA induce the accumulation of IbBBX24 protein in *Fob*-resistant ND98. Anti-HSP was used as a sample loading control.

suppression of *CmBBX24* in chrysanthemum resulted in no obvious morphological variations during vegetative growth (Yang et al., 2014). Therefore, we carefully compared the morphological changes in in vitro–grown wild type versus *IbBBX24-OE* or *IbBBX24-Ri* transgenic plants. The *IbBBX24-OE* plants showed greener, larger, and increased numbers of leaves, whereas the *IbBBX24-Ri* plants exhibited yellower, longer, larger, and reduced numbers of leaves compared with wild-type plants (Supplemental Figures 5A to 5E). Furthermore, the *IbBBX24-OE* and *IbBBX24-Ri* plants had longer roots than wild-type plants, and the internode distance was shorter in the *IbBBX24-Ri* lines than in the other lines (Supplemental Figures 5B and 5F). However, one month after transfer to soil (in both the greenhouse and field), the morphological differences between transgenic and wild-type plants were almost undetectable (Supplemental Figures 5G, 5H, 5J, and 5K). Notably, overexpression of *IbBBX24* led to increased storage root yield (the total weight of storage roots) per plant, whereas knockdown of *IbBBX24* did not obviously affect yields (Supplemental Figures 5I and 5L).

The cultivation of sweet potato, an asexually propagated tuberous root crop species, relies on stem cuttings. *Fob* is primarily spread via the entry of airborne fungal spores into external wounds

(e.g., those from insects) or the invasion of soil-borne spores into the stem cutting incision. We used two methods, mycelial infection and spore infection, to examine the severity of *Fob* infection in transgenic plants.

For the mycelial infection method, pieces of potato dextrose agar (PDA) medium containing *Fob* mycelia were placed onto 1-cm–long wounds on the stems of ND98, Lizixiang (wild type), and *IbBBX24* transgenic plants. Sterile PDA medium was applied simultaneously as a mock treatment. No significant differences in the growth of the wounded stems or the length of the necrotic regions on wounded stems were observed in mock-infected plants (Supplemental Figures 6A, 7A, and 7B). However, at 15-d after inoculation (DAI) with *Fob*, the *IbBBX24-Ri* plants died, their leaves and stems were withered and brown, and the number of diseased leaves and length of the necrotic regions on wounded stems were significantly higher than those of wild-type plants. By contrast, the *Fob*-resistant ND98 and *IbBBX24-OE* plants showed only minor symptoms and sustained normal growth, and the number of diseased leaves and the length of the necrotic regions on wounded stems were significantly lower than those of the wild type (Figure 2A; Supplemental Figures 7A and 7B).

For the spore infection method, cuttings (~25 cm) from 6-week–old ND98, Lizixiang (wild type), and *IbBBX24* transgenic plants were dipped in spore-containing water or sterile water (mock treatment; with 5-cm–long stems from the cutting site dipping into the liquid) and cultivated in sterilized sand irrigated with sterilized Hoagland solution. No significant differences in growth were observed in mock-infected versus untreated plants (Supplemental Figures 6B, 7C to 7E). However, at 5 DAI with *Fob*, most leaves of wild-type and *IbBBX24-Ri* plants began to turn

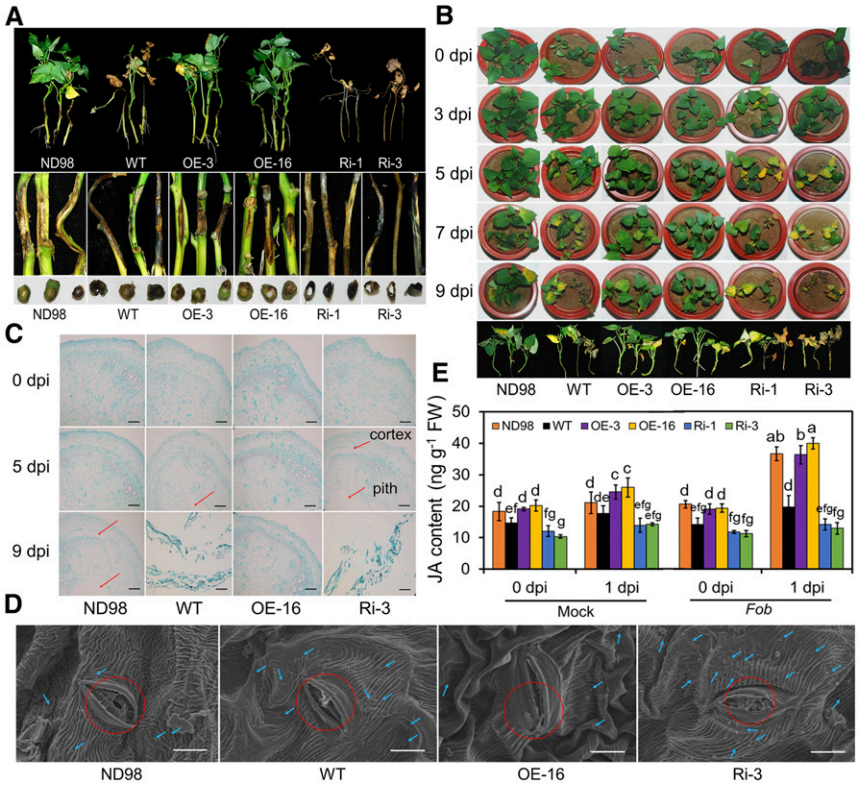

Figure 2. Overexpression of *IbBBX24* Enhances *Fob* Resistance in Sweet Potato.

(A) Development of disease symptoms in *Fob*-resistant line ND98, wild-type (WT), and *IbBBX24* transgenic pot-grown plants after *Fob* inoculation by the mycelia infection method. Sterile PDA tablets (mock, shown in Supplemental Figure 6A) or *Fob* mycelia tablets at the same growth state were placed on a 1-cm–long wound on the stems of plants. Surface and transverse sections of diseased stems are shown. The images were taken at 15 DAI.

(B) Development of disease symptoms in ND98, wild-type (WT), and *IbBBX24* transgenic plants after *Fob* inoculation by the spore infection method. The pot-grown plants were inoculated with water (mock, shown in Supplemental Figure 6B) or an *Fob* spore solution at a density of 1.5×10^7 mL^{-1} for 9 d of treatment.

(C) Histological examination of transverse sections of stems of ND98, wild-type (WT), and *IbBBX24* transgenic plants infected with *Fob* by the spore infection method at 0, 5, and 9 DAI. The red arrows indicate loose cells. Scale bars = 100 μm.

(D) Scanning electron microscopy images of fungus growing in the leaf stomata of ND98, wild-type (WT), and *IbBBX24* transgenic plants infected with *Fob* at 3 DAI by the spore infection method. The red circles indicate fungus growing from the stomata, and the blue arrows indicate *Fob* spores. Scale bars = 10 μm.

(E) JA contents in ND98, wild-type (WT), and *IbBBX24* transgenic plants at 0 DAI and 1 DAI by the spore infection method. The pot-grown plants were inoculated with water (mock, shown in Supplemental Figure 6B) or an *Fob* spore solution at a density of 1.5×10^7 mL^{-1} (*Fob*, shown in Figure 2B) for 9 d of treatment. Leaves located in the same position (the fourth leaf) from three plants were pooled as one replicate. Three biological replicates were performed. Different letters indicate statistically significant differences. Multiple comparisons were calculated by two-way ANOVA followed by Bonferroni post hoc tests ($P < 0.05$). FW, fresh weight.

yellow and fell off, starting from the bottom of the plant and progressing to the top, whereas only a few leaves of ND98 and *IbBBX24-OE* plants displayed these symptoms (Figure 2B). At 9 DAI, the number of diseased leaves and the length of the necrotic regions of stems were significantly reduced in ND98 and *IbBBX24-OE* plants and significantly increased in *IbBBX24-Ri* plants compared with wild-type plants (Supplemental Figures 7C and 7D). Notably, the transgenic plants produced fewer new roots after infection with *Fob* compared with mock-treated plants (Supplemental Figure 7E).

We performed histological analysis to examine the degree of *Fob* damage to the stems of ND98, wild-type, and transgenic plants at 0, 5, and 9 DAI to obtain a before-and-after comparison of disease symptoms. At 5 DAI with *Fob*, the cells in the piths of wild-type and *IbBBX24-Ri* plants were deformed and loosely arranged, whereas the stem structure of ND98 and *IbBBX24-OE* plants remained intact, with compact cells in the pith and cortex (Figure 2C). At 9 DAI with *Fob*, the stems of wild-type and *IbBBX24-Ri* plants exhibited destroyed pith and cortex structures, but these structures displayed much less damage in *IbBBX24-OE* plants (Figure 2C). We then observed the growth of *Fob* on the plants via scanning electron microscopy. Mycelia and spores grew from the stomata of leaves, with more spores observed in *IbBBX24-Ri* plants and fewer spores observed in *Fob*-resistant ND98 and *IbBBX24-OE* plants compared with wild-type plants at 3 dpi (Figure 2D).

Next, we quantified endogenous JA levels in mock- and *Fob*-treated plants. In general, JA was much more abundant in ND98 and *IbBBX24-OE* plants than in wild-type plants under both mock and *Fob* treatment. At 1 DAI with *Fob*, ND98 and *IbBBX24-OE* plants contained higher levels of JA than mock- or *Fob*-infected plants at 0 DAI (Figure 2E). By contrast, *IbBBX24-Ri* plants contained less JA than the controls (Figure 2E). These results indicate that overexpressing *IbBBX24* increases JA contents and *Fob* resistance in the *Fob*-susceptible variety Lizixiang.

JA Inhibits *Fob* Growth and Promotes *Fob* Resistance in Sweet Potato

The exogenous application of MeJA (a stable derivative of JA) activates the defense system against pathogenic organisms in some plant species (Sun et al., 2013; Król et al., 2015; Oliveira et al., 2015). Therefore, we examined whether exogenous MeJA treatment would affect *Fob* growth in sweet potato. We cultured *Fob* mycelia at the same growth period and state on PDA plates containing different concentrations of MeJA. Notably, treatment with higher concentrations of MeJA increasingly inhibited the growth of *Fob* (Supplemental Figures 8A and 8B). In addition, higher concentrations of MeJA inhibited the formation of *Fob* macroconidia (Supplemental Figure 8C). These results indicate that MeJA treatment inhibits the growth of *Fob*.

Because 0.5 mM of MeJA appears to be a relatively low concentration but effectively inhibited the growth of *Fob* (Supplemental Figure 8), we tested the effect of exogenous 0.5-mM MeJA treatment on *Fob* resistance in sweet potato. No significant differences in the growth of sweet potato were observed after exogenous treatment with 0.5 mM of MeJA, as indicated by the phenotypes of aboveground parts and the number of new roots (Supplemental Figure 9). We then applied *Fob* (by the spore infection method) to various genotypes of sweet potato plants that had been treated with or without 0.5 mM of MeJA. Exogenous MeJA treatment effectively slowed the spread of the fungus (Figure 3A). Specifically, at 3 DAI, the leaves of plants not treated with MeJA began to turn yellow from the bottom of the plant, whereas in plants treated with MeJA, the leaves remained green (Figure 3A). In MeJA-treated sweet potato plants at 7 DAI, the number of diseased leaves and the infected regions of the stems decreased by 23% to 51% and 37% to 76%, respectively, compared with mock-treated plants (Figures 3B and 3C). Collectively, our data indicate that MeJA treatment promotes *Fob* resistance in sweet potato.

IbBBX24 Regulates the Transcription of Genes Involved in the JA Pathway

To better understand how *IbBBX24*-mediated *Fob* resistance is regulated, we performed RNA-seq analysis of Lizixiang (wild type) and *IbBBX24* transgenic plants (OE-16 and Ri-3) at 1 DAI after infection with *Fob*. Because cultivated sweet potato ($2n = B_1B_1B_2B_2B_2B_2 = 6x = 90$) is a highly heterozygous and generally self-incompatible autohexaploid, its genome is difficult to assemble and is highly polymorphic (Liu, 2017). To select an appropriate reference genome, we aligned the RNA-seq reads to previously released sweet potato genome sequences (Hirakawa et al., 2015; Yang et al., 2017; Wu et al., 2018). Among our RNA-seq reads, 72.99%, 78.09%, 73.82%, and 79.09% were successfully aligned to the genomes of wild sweet potato relatives *Ipomoea trifida* 0431-1 ($2n = 2x = 30$; Hirakawa et al., 2015), *I. trifida* NCNSP0306 ($2n = 2x = 30$; Wu et al., 2018), and *Ipomoea triloba* NCNSP0323 ($2n = 2x = 30$; Wu et al., 2018), and the sweet potato variety Taizhong 6 ($2n = 6x = 90$; Yang et al., 2017), respectively (Supplemental Table 2). As the highest percentage of reads was mapped to the Taizhong 6 genome, and because the Taizhong 6 genome was the only published hexaploid sweet potato genome, we used this genome sequence for further RNA-seq analysis.

We used RNA-seq to examine the expression of 57,377 genes in overexpression line OE-16, RNAi line Ri-3, and wild-type plants (Figure 4A; Supplemental Figure 10). Further comparisons of the RNA-seq data of OE-16, Ri-3, and wild-type plants at 1 DAI (with a threshold of *False Discovery Rate* [*FDR*] < 0.05) revealed 19,777 DEGs. Compared with the wild type, 6,370 upregulated and 6,054 downregulated genes were identified in OE-16, whereas 7,084 upregulated and 9,248 downregulated genes were identified in Ri-3 (Figure 4B). In addition, 2,470 genes were upregulated in OE-16 but downregulated in Ri-3, and 1,407 genes were downregulated in OE-16 but upregulated in Ri-3 after infection with *Fob* (Figure 4B; Supplemental Data Set 2). Therefore, these 3,877 genes were regulated in an opposite manner in the overexpression and knockdown lines of *IbBBX24*. We functionally annotated and classified these 3877 genes using the Kyoto Encyclopedia of Genes and Genomes (KEGG) database. KEGG enrichment analysis revealed that these DEGs were enriched in processes such as protein processing in endoplasmic reticulum (ath04141), plant hormone signal transduction (ath04075), biosynthesis of amino acids (ath01230), and plant–pathogen interaction (ath04626; Supplemental Figure 11A).

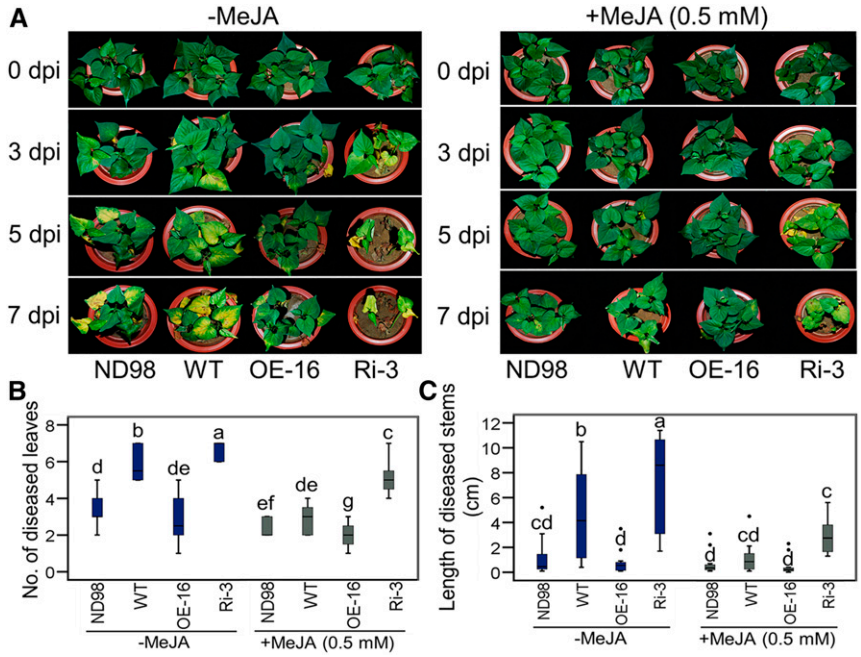

Figure 3. Effects of MeJA Treatment on *Fob* Resistance in Sweet Potato.

(A) Development of disease symptoms in *Fob*-resistant line ND98, wild-type (WT), and *IbBBX24* transgenic plants after *Fob* inoculation by the spore infection method with or without MeJA treatment. Pot-grown plants were inoculated with *Fob* spore solution at a density of 1.5×10^7 mL^{-1} for 7 d of treatment. Plants were irrigated with 100 mL of 0 mM or 0.5 mM of MeJA solution per pot once a day. The disease phenotypes were photographed at 0, 3, 5, and 7 DAI. The experiment was independently repeated four times with three plants per replicate.

(B) and **(C)** Statistical analysis of the number of diseased leaves **(B)** and the length of the necrotic regions of stems **(C)** of ND98, wild-type (WT), and *IbBBX24* transgenic plants at 7 DAI by the spore infection method with or without MeJA treatment. The values represent ±SD ($n = 12$) from four independent biological replicates with three plants per replicate. The dots represent outlier points. Different letters indicate statistically significant differences. Multiple comparisons were calculated by two-way ANOVA followed by Bonferroni post hoc tests ($P < 0.05$).

Notably, based on sequence similarity with Arabidopsis homologs, regulatory genes involved in JA biosynthesis and signaling, such as encoding lipoxygenases (Oliw and Hamberg, 2017), encoding allene oxide synthase (Park et al., 2002), encoding OPDA reductase3 (Schaller et al., 2000), *IbMYC2* (Dombrecht et al., 2007), and *IbCHI* (encoding the antimicrobial protein chitinase; Ebrahim et al., 2011) were upregulated in OE-16 but downregulated in Ri-3 versus the wild type after *Fob* infection (Figure 4C; Supplemental Data Set 2). *IbJAZ10* was downregulated in OE-16 but upregulated in Ri-3 versus wild type after *Fob* infection (Figure 4C; Supplemental Data Set 2). RT-qPCR demonstrated that the expression levels of *IbMYC2* and *IbCHI* were significantly higher, but the expression level of *IbJAZ10* was significantly lower, in *IbBBX24-OE* plants compared with both wild-type and *IbBBX24-Ri* plants before and after infection (Figure 4D).

JA-mediated signaling activates the transcription of pathogen defense genes and regulates the production of reactive oxygen species (ROS) and lignin (Denness et al., 2011). Higher concentrations of ROS dramatically promote oxidative damage in plants under stress (Apel and Hirt, 2004), while lignin and phenols play essential roles in the defense response to invading pathogens (Nicholson and Hammerschmidt, 1992; Brisson et al., 1994). After *Fob* infection, DEGs such as pathogenesis-related genes, disease-resistance genes (Nepal et al., 2017), late blight resistance genes (Pel et al., 2009), genes encoding leucine-rich repeat domain-containing proteins (Hu et al., 2018), ROS scavenging-related genes (Apel and Hirt, 2004), and lignin/cell wall synthesis-related genes (Douchkov et al., 2016) were significantly upregulated in OE-16 but downregulated in Ri-3 compared with the wild type (Supplemental Figure 12). We measured pathogen defense-related indices in wild-type and *IbBBX24* transgenic plants after infection. Superoxide dismutase (SOD) and peroxidase (POD) activity and total phenolic and lignin contents were significantly higher in the *IbBBX24-OE* lines but lower in the *IbBBX24-Ri* lines compared with the wild type (Supplemental Figures 13A, 13B, 13E, and 13F). By contrast, malondialdehyde (MDA) and hydrogen peroxide (H_2O_2) contents were significantly lower in the *IbBBX24-OE* lines and higher in the *IbBBX24-Ri* lines compared with the wild type (Supplemental Figures 13C and 13D). These data indicate that *IbBBX24* affects the transcription of genes involved in the JA-mediated defense pathway in sweet potato.

Genome-wide Binding Analysis of IbBBX24 by Chromatin Immunoprecipitation Sequencing

Next, we explored the target genes of IbBBX24 by performing chromatin immunoprecipitation sequencing (ChIP-seq) assays using specific polyclonal anti-IbBBX24 antibodies in line OE-16 at

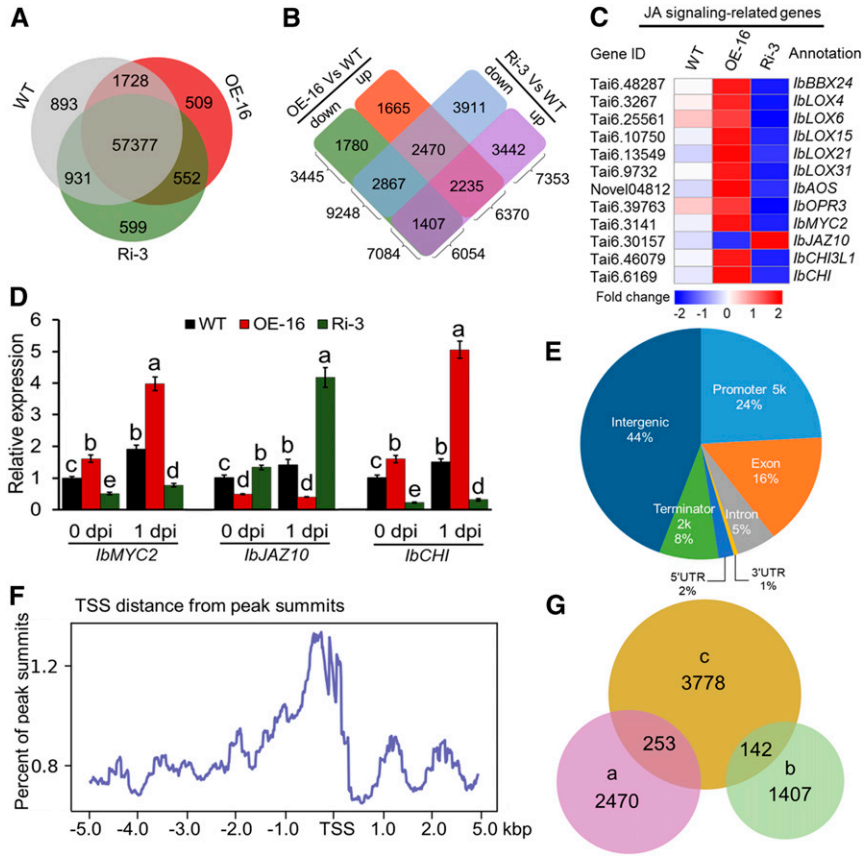

Figure 4. Genome-wide Analysis of the Role of the IbBBX24 Regulon in the *Fob* Response.

(A) Venn diagram of the number of expressed genes in OE-16, Ri-3, and wild type (WT) at 1 DAI with *Fob* by RNA-seq.
(B) The number of DEGs among OE-16, Ri-3, and wild type (WT) at 1 DAI with *Fob* by RNA-seq.
(C) Heat map of DEGs involved in the JA pathway based on RNA-seq analysis of OE-16 and Ri-3 at 1 DAI of *Fob*. Higher transcript levels are shown in red (0 to 2), and lower transcript levels are shown in blue (−2 to 0). WT, wild type.
(D) Relative expression levels of *IbMYC2*, *IbJAZ10*, and *IbCHI* in wild-type (WT) and *IbBBX24* transgenic plants at 0 DAI and 1 DAI with *Fob*. The values were determined by RT-qPCR from three biological replicates consisting of pools of five plants. The error bars indicate ±SD ($n = 3$). Different lowercase letters indicate a significant difference at $P < 0.05$ based on Student's *t* test.
(E) Distribution of IbBBX24 binding regions in the sweetpotato genome. ChIP was performed in line OE-16 at 1 DAI with *Fob* with anti-IbBBX24 antibody. Promoter 5-k region, −5 kb to TSS; terminator 2-kb region, 2 kb downstream of the terminator.
(F) Peak distance from the TSS of *IbBBX24*. The peaks were highly enriched from −1 kb to 0 from the TSS.
(G) Venn diagram showing the number and overlap of DEGs detected by RNA-Seq and ChIP-Seq at 1 DAI with *Fob*. a, 2,470 DEGs were upregulated in OE-16 and downregulated in Ri-3 compared with the wild type, as detected by RNA-seq; b, 1,407 DEGs were downregulated in OE-16 and upregulated in Ri-3 line compared with the wild type, as detected by RNA-seq; c, 3,778 putative targets containing peaks associated with a gene model detected by ChIP-seq.

1 DAI after *Fob* infection. We mapped the sequencing reads of ChIP DNA to the Taizhong 6 genome using BWA v0.7.12 (Langmead et al., 2009; Yang et al., 2017). We identified 1,427,515 uniquely mapped reads, which were distributed throughout the Taizhong 6 genome. In total, 7,930 binding peaks of IbBBX24 were detected with a Q-value < 0.05 for the ChIP-seq data sets (Supplemental Data Set 3). Approximately 56% of the 7,930 IbBBX24 binding peaks were located in the genic regions of 3,778 genes. Of these, 24% were located in promoter regions (−5 kb to the transcription start site [TSS]), 16% in exon regions, 5% in intron regions, 2% in 5′-UTRs, 1% in 3′-untranslated regions (UTRs), and 8% in terminator regions (2 kb downstream of the terminators; Figure 4E). The binding peaks were significantly concentrated within the 1,000-bp region upstream of the TSS, and 602 peaks in this region were assigned to 534 genes (Figure 4F). The 3,778 genes were functionally annotated and classified using the KEGG database. KEGG enrichment analysis revealed that they were mainly enriched in the pathways' oxidative phosphorylation (ath00190), plant hormone signal transduction (ath04075), biosynthesis of amino acids (ath01230), protein processing in the endoplasmic reticulum (ath04141), and plant–pathogen interactions (ath04626; Supplemental Figure 11B).

As described above, our RNA-seq analyses identified 2,470 DEGs that were upregulated in OE-16 but downregulated in Ri-3 and 1,407 DEGs that were downregulated in OE-16 but upregulated in Ri-3 after *Fob* infection (Figure 4B). A comparison of our

RNA-seq results with the ChIP-seq data showed that of the IbBBX24-regulated genes, 253 of the 2,470 DEGs and 142 of the 1,407 DEGs described above were bound by IbBBX24 in vivo (Figure 4G; Supplemental Data Set 4), suggesting that their expression is directly regulated by IbBBX24. Of the 395 direct targets of IbBBX24, 64% were located upstream of the TSS (including 10% located in the region 1 kb upstream of the TSS), 8% were located within gene bodies, and 28% were located downstream of coding sequences (Supplemental Data Set 4). Next, we selected two putative direct targets of IbBBX24, *IbCHI* and *IbCRK* (encoding a CDPK-related kinase), to verify that they are indeed directly regulated by IbBBX24. IbBBX24 binding peaks were located immediately upstream of the TSS of both genes. Yeast one-hybrid (Y1H) assays indicated that IbBBX24 directly bound to their promoters in yeast cells, and transient dual-luciferase assays showed that IbBBX24 strongly activated *IbCHIpro-LUC* but inhibited *IbCRKpro-LUC* expression in sweet potato protoplasts (Supplemental Figure 14). Collectively, combining our genome-wide analysis of IbBBX24 binding to DNA and differences in RNA expression in *IbBBX24*-overexpressing and -silenced lines, we conclude that 253 and 142 genes are likely direct targets of activation and repression by IbBBX24, respectively.

IbBBX24 Participates in JA-Mediated Disease Resistance by Binding to the Promoters of *IbJAZ10* and *IbMYC2*

Given the finding that overexpression of *IbBBX24* increases JA contents and *Fob* resistance in the *Fob*-susceptible variety Lizixiang (Figure 2) and that *IbBBX24* affects the transcription of genes involved in the JA-mediated defense pathway (Figure 4C), it was interesting to note that *IbJAZ10* and *IbMYC2*, two important components in the JA-signaling pathway, are direct target genes of IbBBX24 (Supplemental Data Set 4). To further verify their regulation by IbBBX24, we examined the expression of *IbJAZ10* and *IbMYC2* in wild type, OE-16, and Ri-3 plants before and after infection with *Fob*. RT-qPCR analysis indicated that *IbJAZ10* was downregulated by IbBBX24 after infection, whereas *IbMYC2* was upregulated by this transcription factor (Figures 5A and 5B), which is consistent with our RNA-seq data (Supplemental Data Set 2).

The finding that IbBBX24 interacts with genomic sequences located upstream of the coding sequences of *IbJAZ10* and *IbMYC2* suggests that IbBBX24 directly regulates these genes by binding to their promoters (Figures 5C and 5D). We performed electrophoretic mobility shift assays (EMSAs) to further verify the binding of IbBBX24 to these promoters. Indeed, in Arabidopsis, BBX proteins bind to the T/G-box elements in the promoters of their target genes (Xu et al., 2016, 2018). Although analysis of the *IbJAZ10* promoter sequence failed to reveal the presence of a typical T/G-box, in the EMSA, 6His-tagged IbBBX24 bound to a 51-bp promoter fragment of *IbJAZ10* (~105 bp upstream the ATG start codon) in vitro (Figure 5E). We also identified two typical T/G-boxes in the *IbMYC2* promoter. To investigate whether IbBBX24 binds to the *IbMYC2* promoter through these T/G-boxes, we performed EMSAs using a 62-bp wild-type probe and mutant probes in which one or both of the T/G-boxes were mutated (Figure 5F). IbBBX24 directly bound to the wild-type probe. However, the mutation of either T/G-box1 or T/G-box2 decreased IbBBX24 binding, whereas the mutation of both T/G-box1 and T/G-box2 totally abolished the binding of IbBBX24 to the *IbMYC2* promoter probe (Figure 5F). Together, these data indicate that both T/G-box1 and T/G-box2 are important for mediating IbBBX24 binding to the *IbMYC2* promoter.

We performed transient dual-luciferase assays in sweet potato protoplasts to investigate how IbBBX24 regulates the expression of *IbJAZ10* and *IbMYC2*. When *IbJAZ10pro-LUC* was cotransformed with 35S-IbBBX24, the *IbJAZ10* promoter was inhibited by the presence of IbBBX24. By contrast, when *IbMYC2pro-LUC* was cotransformed with 35S-IbBBX24, the *IbMYC2* promoter was activated by the presence of IbBBX24 (Figures 5G and 5H). Collectively, our data demonstrate that IbBBX24 directly represses *IbJAZ10* but activates *IbMYC2* expression by binding to their promoters.

Physical Interaction between IbBBX24 and IbJAZ10

The Arabidopsis homolog BBX24 physically interacts with CONSTITUTIVE PHOTOMORPHOGENIC1, ELONGATED HYPOCOTYL5, and DELLA proteins (Yan et al., 2011; Jiang et al., 2012; Crocco et al., 2015). To explore the possible interacting partners of IbBBX24 involved in *Fob* resistance in sweet potato, we screened a yeast two-hybrid (Y2H) library constructed using RNA from sweet potato leaves. Because IbBBX24 acted as a transcriptional activator in yeast cells, and 133 amino acid residues from the carboxy-terminus were required for its transactivation activity (Figure 6A), we used 98 amino acid residues from the N terminus of IbBBX24 (BD-IbBBX24^{N98}), which includes the two B-box domains, as the bait in Y2H screens. This effort led to the identification of 17 putative IbBBX24-interacting proteins (Supplemental Table 3), including IbJAZ10 (Figure 6A).

To verify the interaction between IbBBX24 and IbJAZ10 in plant cells, we conducted bimolecular fluorescence complementation (BiFC), firefly luciferase complementation imaging (LCI), and coimmunoprecipitation (co-IP) assays in *N. benthamiana* leaves. The coexpression of n-terminal yellow fluorescent protein (nYFP)-IbBBX24 and IbJAZ10-cYFP led to clear YFP signals in the nucleus, and the coexpression of nLUC-IbBBX24 and IbJAZ10-cLUC resulted in strong LUC activity in *N. benthamiana* leaves. By contrast, no signal (BiFC) and only background levels of LUC activity (LCI) were observed in the negative controls (Figures 6B and 6C). In a co-IP assay, IbJAZ10-Myc was coprecipitated by anti-HA antibody using total proteins extracted from *N. benthamiana* leaves co-expressing HA-IbBBX24 and IbJAZ10-Myc, but not using total proteins extracted from control leaves expressing IbJAZ10-Myc alone (Figure 6D). Together, our data demonstrate that IbBBX24 physically interacts with IbJAZ10 in vivo.

IbBBX24 Enhances the DNA Binding Activity of IbMYC2 by Releasing It from Suppression by IbJAZ10

We performed Y2H assays to identify the domains of IbJAZ10 responsible for interactions with IbMYC2 and IbBBX24. Both the ZIM domain and Jas domain of IbJAZ10 interacted with IbMYC2, whereas the Jas domain of IbJAZ10 interacted with both IbBBX24 and IbCOI1 in yeast cells (Figure 7A). Indeed, the Jas domain of

JAZ proteins interacts with COI1 (Melotto et al., 2008). The Jas domain also mediates the interaction of JAZ proteins with MYC2 (Chini et al., 2009; Pauwels and Goossens, 2011; Goossens et al., 2015).

Next, we asked how IbJAZ10 and IbBBX24 affect the transcriptional activity of IbMYC2. Tomato MYC2 binds to the promoters of the NAC transcription factor gene *JA2L* and the ERF transcription factor gene *ERF.C3* through the consensus CACATG element (Du et al., 2017). Based on our RNA-seq data, we identified a NAC transcription factor gene in sweet potato, *IbNAC72*, whose expression was activated by IbBBX24 (Supplemental Data Set 2). However, *IbNAC72* was not bound by IbBBX24 in vivo, suggesting that IbBBX24 activates *IbNAC72* indirectly. Notably, the *IbNAC72* promoter contains a typical CACATG element. We thus asked whether the expression of *IbNAC72* is regulated by IbMYC2. We performed transient dual-luciferase assays using sweet potato protoplasts and a reporter construct in which the expression of the *LUC* reporter gene was driven by the *IbNAC72* promoter. The coding sequences of *IbMYC2*, *IbJAZ10*, and *IbBBX24* were cloned separately into pGreenII 62-SK as effectors. LUC activity analysis indicated that IbMYC2 directly activated the *IbNAC72* promoter (Figure 7B). However, when IbJAZ10 was co-expressed with

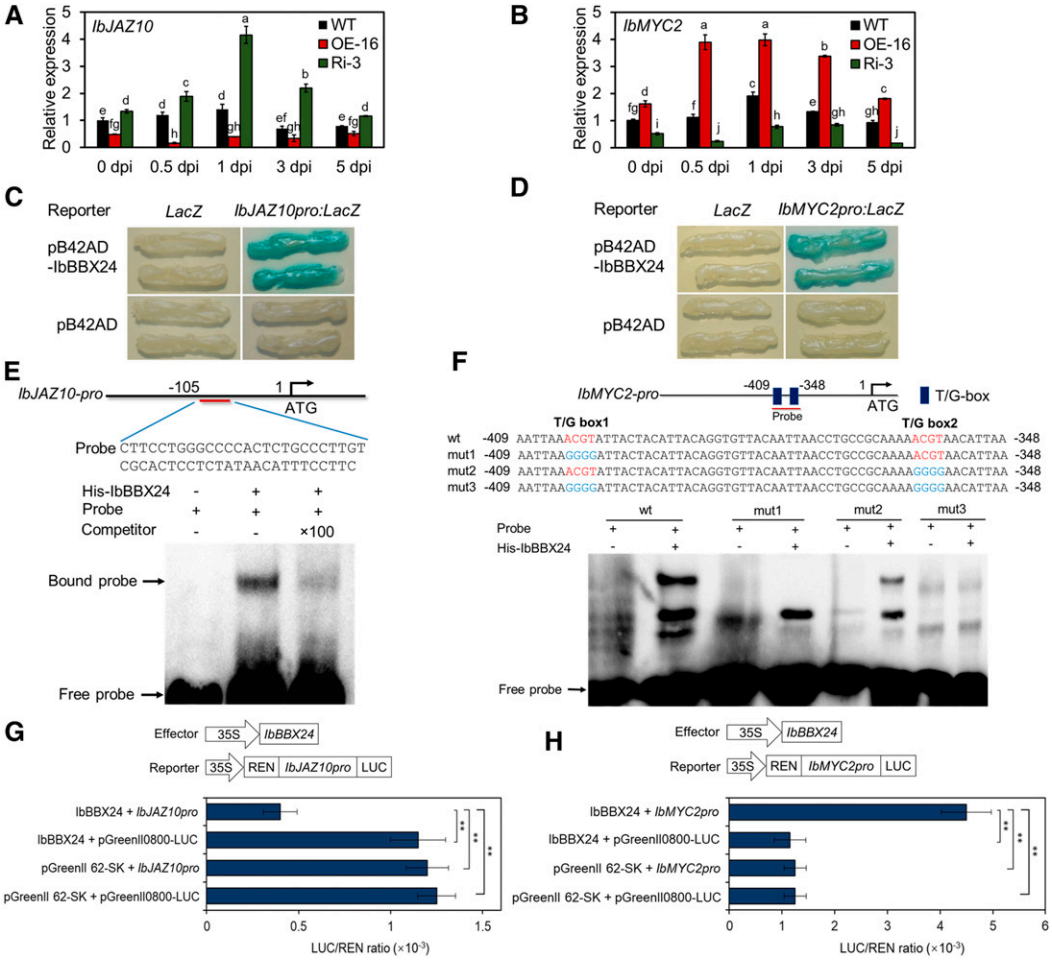

Figure 5. IbBBX24 Regulates *IbJAZ10* and *IbMYC2* Expression by Binding Directly to Their Promoters.

(A) and **(B)** Expression analysis of *IbJAZ10* **(A)** and *IbMYC2* **(B)** in *IbBBX24* transgenic and wild-type (WT) plants at different DAI with *Fob* by the spore infection method. The values were determined by RT-qPCR from three biological replicates consisting of pools of three plants. The error bars indicate ±SD ($n = 3$). Different lowercase letters indicate a significant difference at $P < 0.05$ based on Student's *t* test.

(C) and **(D)** Y1H assays of IbBBX24 binding to the *IbJAZ10* and *IbMYC2* promoters.

(E) Using EMSAs, it was found that the recombinant protein 6His-IbBBX24 retarded the shift of the probe, indicating that IbBBX24 binds to the *IbJAZ10* promoter. 100× indicates the usage of excess nonlabeled probe as a competitor. "+" and "−" indicate presence and absence, respectively.

(F) EMSAs using 6His-IbBBX24 and wild-type (wt) or various mutated versions of the *IbMYC2* promoter subfragments as probes. The terms "mut1," "mut2," and "mut3" stand for mutated probes in which the various T/G-box "ACGT" motifs were replaced with "GGGG."

(G) and **(H)** IbBBX24 inhibits *IbJAZ10*pro-LUC **(G)** but activates *IbMYC2*pro-LUC **(H)** activity, as determined by dual-LUC assays in sweetpotato protoplasts. The expression level of REN was used as an internal control. The LUC/REN ratio represents the relative activity of the *IbJAZ10* promoter. Data are values from four independent experiments. The error bars indicate ±SD ($n = 4$). $^{**}P < 0.01$; Student's *t* test.

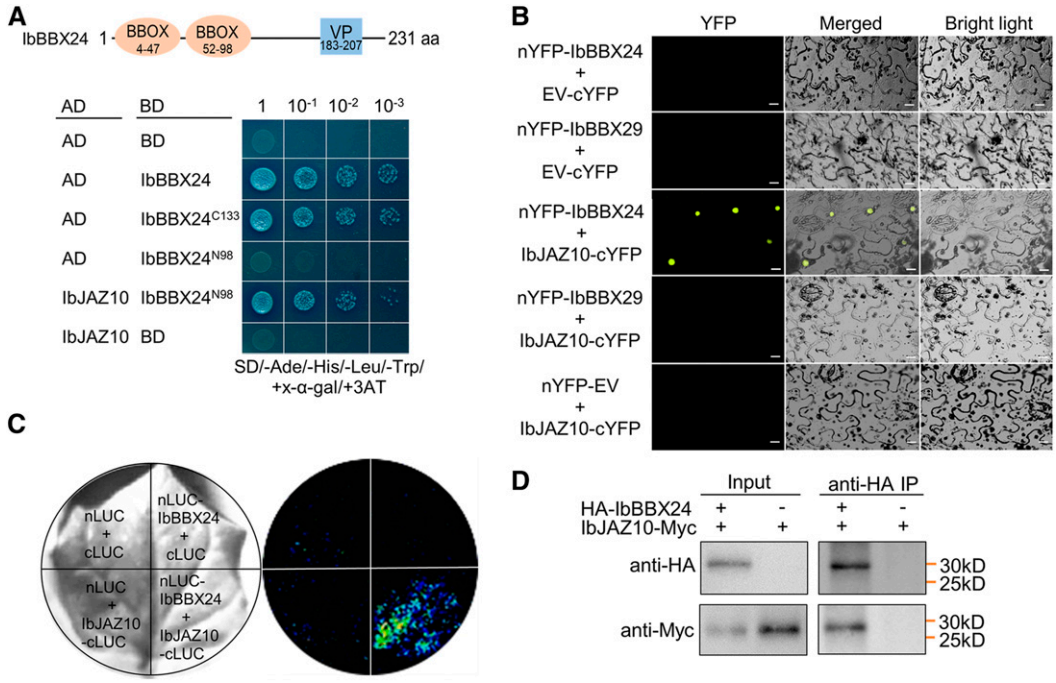

Figure 6. Interaction of IbBBX24 with IbJAZ10 In Vitro and In Vivo.

(A) The B-box domain of IbBBX24 is necessary and sufficient for interaction with IbJAZ10 in a Y2H system. BD-IbBBX24^{N98} contains IbBBX24 amino acid residues 1 to 98, whereas BD-IbBBX24^{C133} contains amino acid residues 99 to 231. Yeast cells were plated onto SD/−Ade/−His/−Leu/−Trp + 3 mM of 3AT medium to screen for possible interactions.

(B) Confirmation of the interaction of IbBBX24 and IbJAZ10 by BiFC in *N. benthamiana* leaf epidermal cells, as shown by a yellow fluorescent signal. The N terminus of YFP was respectively fused to IbBBX24 and IbBBX29, while the C terminus of YFP was fused to IbJAZ10. IbBBX29 from the BBX protein family was used as a related noninteracting protein for a negative control. The images were observed under a confocal microscope 2 d later. EV, empty vector. Scale bars = 10 μm.

(C) LCI assay showing that IbBBX24 interacts with IbJAZ10. The N terminus of LUC was fused to IbBBX24, and the C terminus of LUC was fused to IbJAZ10. The images were observed using chemiluminescence imaging 2 d later.**(D)** In vivo interaction between IbBBX24 and IbJAZ10, as revealed by the co-IP assay. Total proteins from *N. benthamiana* leaf cells expressing HA-IbBBX24 and IbJAZ10-Myc. Total proteins were extracted and incubated with anti-HA agarose beads. Proteins before (input) and after IP were detected with anti-HA and anti-Myc antibodies.

IbMYC2, *LUC* expression significantly decreased, indicating that IbJAZ10 inhibits the trans-activation activity of IbMYC2. Moreover, when we expressed IbBBX24 together with IbJAZ10 and IbMYC2 in sweet potato protoplasts, *LUC* expression again increased (Figure 7B), suggesting that IbBBX24 enhances the ability of IbMYC2 to regulate its target gene. In addition, IbBBX24 promoted IbMYC2 activity in the absence of transiently expressed IbJAZ10 (Figure 7B), perhaps due to the suppression of endogenous JAZ activity by IbBBX24. Together, our data indicate that IbJAZ10 inhibits the trans-activation activity of IbMYC2, but IbBBX24 relieves this inhibition.

To further dissect the molecular mechanisms underlying how IbBBX24 regulates IbBBX24 activity, we performed EMSAs using 6His-tagged IbJAZ10, IbBBX24, and IbMYC2 recombinant proteins and a 30-bp promoter fragment of *IbNAC72* containing the CACATG element. As expected, 6His-IbMYC2 bound to the wild-type promoter fragment of *IbNAC72*, but not to the mutant probe in which CACATG was mutated to GGGGGG (Figure 7C). However, the addition of IbJAZ10 abolished the binding of IbMYC2 to the wild-type *IbNAC72* promoter, which is consistent with the finding that JAZ proteins inhibit the binding activity of transcription factors involved in JA signaling (Song et al., 2011; Qi et al., 2015; Zhang et al., 2015). The addition of IbBBX24 together with IbJAZ10 and IbMYC2 restored the binding of IbMYC2 to the *IbNAC72* promoter (Figure 7C). These results, together with the finding that both IbMYC2 and IbBBX24 interact with the Jas domain of IbJAZ10 (Figure 7A), suggest that the presence of IbBBX24 releases IbMYC2 from IbJAZ10, thus allowing IbMYC2 to bind to its target gene promoter. Collectively, our data demonstrate that IbBBX24 suppresses the inhibitory activity of IbJAZ10 toward IbMYC2, thereby leading to the activation of IbMYC2.

Overexpression of *IbJAZ10* Decreases *Fob* Resistance in Tobacco

JAZ proteins act as repressors of JA signaling, and the roles of JAZ proteins in plant responses to biotic stress have been extensively studied (Demianski et al., 2012; Yamada et al., 2012; de Torres Zabala et al., 2016; Thatcher et al., 2016; Ortigosa et al., 2019). To investigate the role of IbJAZ10 in *Fob* resistance, we overexpressed *IbJAZ10* in tobacco cv Wisconsin 38 (W38), because W38 can also be infected by Fusarium wilt fungus (Yun et al., 1996; Ntui

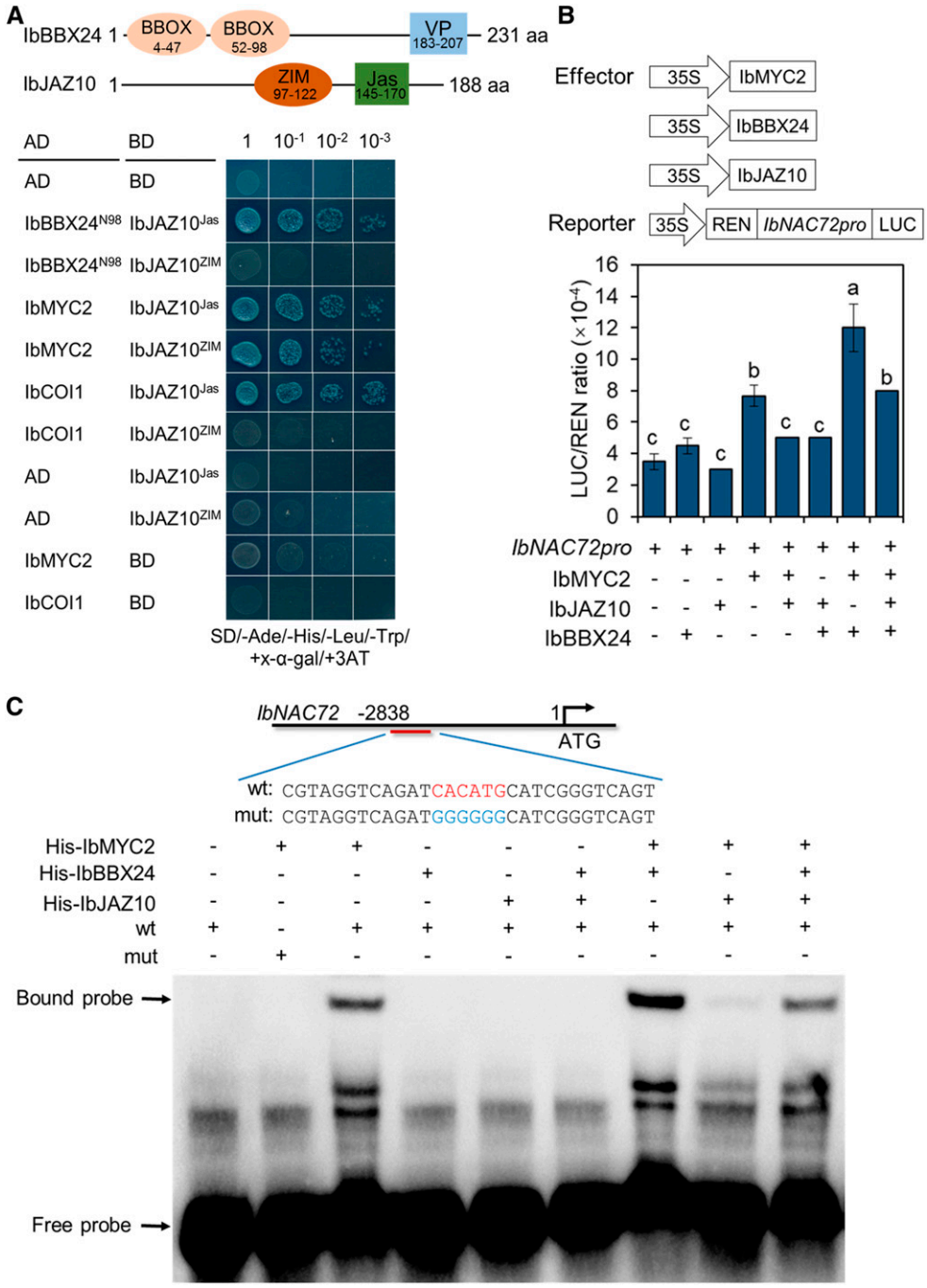

Figure 7. IbBBX24 Enhances the DNA Binding Activity of IbMYC2 by Releasing It from Suppression by IbJAZ10.

(A) Y2H analysis showing that IbJAZ10 interacts with IbBBX24, IbMYC2, and IbCOI1. Yeast cells were plated onto SD/-Ade/-His/-Leu/-Trp and 3 mM 3AT medium for stringent screening of possible interactions.

(B) Interaction of IbMYC2, IbJAZ10, and IbBBX24 with the *IbNAC72* promoter, as determined by dual-LUC assays in sweetpotato protoplasts. The expression level of REN was used as an internal control. The LUC/REN ratio represents the relative activity of the *IbNAC72* promoter. Data are values from three independent experiments. The error bars indicate $\pm$SD ($n = 3$). Different lowercase letters indicate a significant difference at $P < 0.05$ based on Student's *t* test.

(C) EMSA showing that the DNA binding of IbMYC2 is suppressed by IbJAZ10 but stimulated by IbBBX24 in vitro. Biotin-labeled probes were incubated with various combinations of the same amount of purified 6His-IbBBX24, 6His-IbMYC2, and 6His-IbJAZ10 proteins, and the free and bound DNAs were separated on an acrylamide gel. mut, mutated probe in which the G-box motif CACATG was replaced with GGGGGG; wt, wild type.

et al., 2011). We examined the transcript levels of *IbJAZ10* in various transgenic lines by RT-qPCR and screened four independent transgenic lines (L4, L7, L18, and L25) in which *IbJAZ10* was dramatically overexpressed (Figure 8C) for *Fob* resistance. Under normal growth conditions, these *IbJAZ10-OE* lines exhibited significantly smaller leaves, longer but thinner stems, and shorter roots than wild-type W38 plants (Figures 8A to 8F). Upon infection with *Fob* spores, the *IbJAZ10-OE* lines showed a severe *Fob*-susceptible phenotype, with wilted leaves and stems, whereas control W38 plants maintained normal growth and formed new roots (Figures 8G and 8H). Consistent with this finding, the number of diseased leaves and the length of the necrotic regions of stems were significantly greater in *IbJAZ10-OE* plants compared with wild-type plants (Figures 8I and 8J). Taken together, these results indicate that IbJAZ10 functions as a negative regulator of the *Fob* response in plants.

DISCUSSION

Accumulating evidence indicates that the immunity hormone JA regulates diverse plant defense responses and various developmental processes by interacting with other signaling pathways (Zhai et al., 2017; Yang et al., 2019). The JAZ-MYC module is extensively involved in the crosstalk between JA signaling and

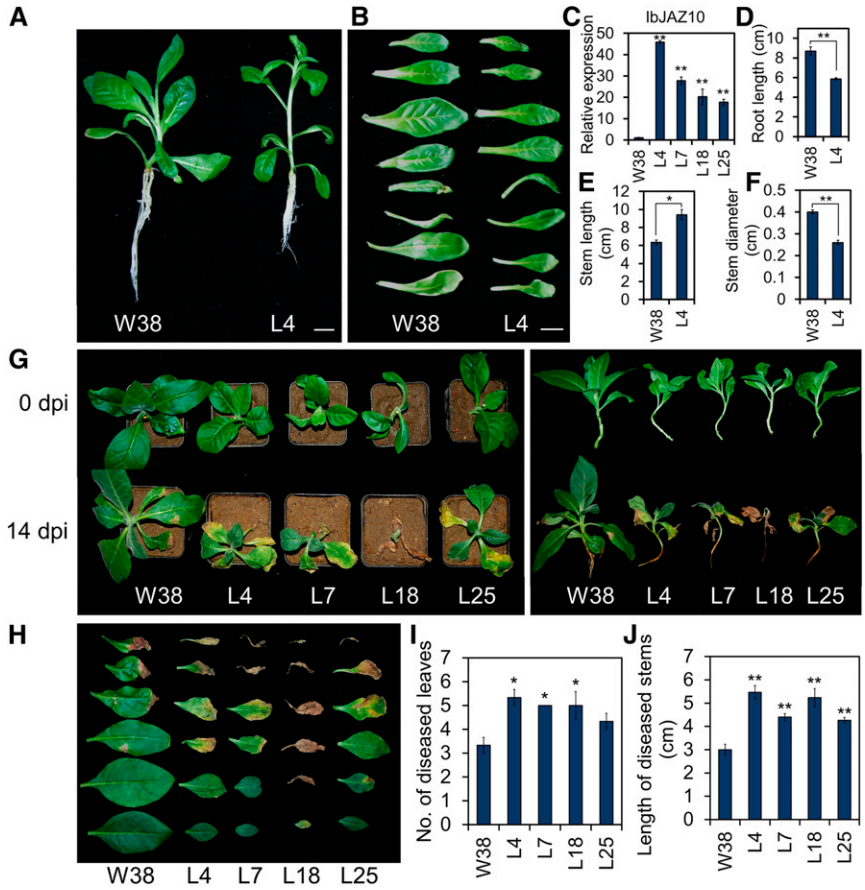

Figure 8. Overexpression of *IbJAZ10* in Tobacco Increases Plant Susceptibility to *Fob.*

(A) Phenotypes of one-month–old L4 and W38 tobacco plants grown in half strength MS medium. Scale bar = 1.5 cm.

(B) Leaf phenotypes of one-month–old L4 and W38 plants grown in half strength MS medium. Scale bar = 1.5 cm.

(C) Transcript levels of *IbJAZ10* in W38 and transgenic tobacco lines. The results are expressed as relative values with respect to W38, which was set to 1.0. The values were determined by RT-qPCR from three biological replicates consisting of pools of three plants. The error bars indicate ±SD ($n = 3$). $^{**}P < 0.01$; Student's *t* test.

(D) to **(F)** Root length **(D)**, stem length **(E)**, and stem diameter **(F)** of one-month–old L4 and W38 plants grown in half strength MS medium. The error bars indicate ±SD ($n = 3$). $^{*}P < 0.05$; $^{**}P < 0.01$; Student's *t* test.

(G) Development of plant disease symptoms in W38 and *IbJAZ10* transgenic plants after *Fob* inoculation. W38 and *IbJAZ10* transgenic plants were inoculated with *Fob* spores at a density of 1.5×10^7 mL^{-1} for 14 d.

(H) Development of disease symptoms in leaves of W38 and *IbJAZ10* transgenic plants after *Fob* inoculation. W38 and *IbJAZ10* transgenic plants were inoculated with *Fob* spores at a density of 1.5×10^7 mL^{-1} for 14 d.

(I) and **(J)** Number of diseased leaves **(I)** and the length of the necrotic regions of stems **(J)** in W38 and *IbJAZ10* transgenic plants at 14 DAI. The error bars indicate ±SD ($n = 9$). $^{*}P < 0.05$; $^{**}P < 0.01$; Student's *t* test.

other signaling pathways. For example, JAZ1 and JAZ4 interact with INDUCER OF CBF EXPRESSION1 (ICE1) and ICE2 to inhibit the ICE-CBF signaling pathway (Hu et al., 2017), and TOE1 and TOE2 interact with a subset of JAZ proteins (JAZ1, JAZ3, JAZ4, and JAZ9) to regulate JA-mediated flowering (Zhai et al., 2015). In addition, DELLAs, which are key repressors of GA signaling, modulate JA signaling by interacting with JAZs to enhance the ability of MYC2 to regulate its target genes (Hou et al., 2010). In this study, we demonstrated that the BBX family transcription factor IbBBX24 participates in the JA pathway by modulating the JAZ-MYC module in sweet potato. IbBBX24 represses *IbJAZ10* expression but activates *IbMYC2* expression by binding directly to their promoters (Figure 5). In addition, IbBBX24 physically interacts with IbJAZ10, thus relieving its inhibition of IbMYC2 activity (Figure 7). Therefore, our study demonstrates that IbBBX24 mediates the JA-signaling pathway and Fusarium wilt resistance in sweet potato by regulating target gene expression and protein–protein interactions (Figure 9).

Although JA plays an important role in plant defense responses to necrotrophic and hemibiotrophic fungal pathogens, the interactions between plants and pathogens are far more complex than previously thought (Yan and Xie, 2015). Pathogens may secrete toxins and inject virulence effector proteins into host cells, which target components of JA signaling, thus suppressing or evading host defense responses (Cui et al., 2010; Thatcher et al., 2012; Jiang et al., 2013; Zhu et al., 2013; Cole et al., 2014; Gimenez-Ibanez et al., 2014). For example, *Pseudomonas syringae* pv *Tomato* DC3000 secretes coronatine (a JA-Ile mimic) and HopZ1a (a virulence effector protein) to destabilize JAZ repressor proteins and inappropriately activate the JA-signaling pathway in host cells (Feys et al., 1994; Kloek et al., 2001; Laurie-Berry et al., 2006; Jiang et al., 2013). This sabotages SA-dependent host defense in wild-type plants, leading to increased susceptibility to *Pseudomonas syringae* pv *Tomato* DC3000 (Kloek et al., 2001; Laurie-Berry et al., 2006). Some *F. oxysporum* f. sp, such as *F. oxysporum* f. sp *conglutinans* and *F. oxysporum* f. sp *matthioli* (*Fom*), produce jasmonate-related metabolites and use them as effectors to promote infection in Arabidopsis (Thatcher et al., 2009; Cole et al., 2014; Yan and Xie, 2015). In addition, *F. oxysporum* hijacks COI1-mediated JA signaling in host cells to promote plant susceptibility

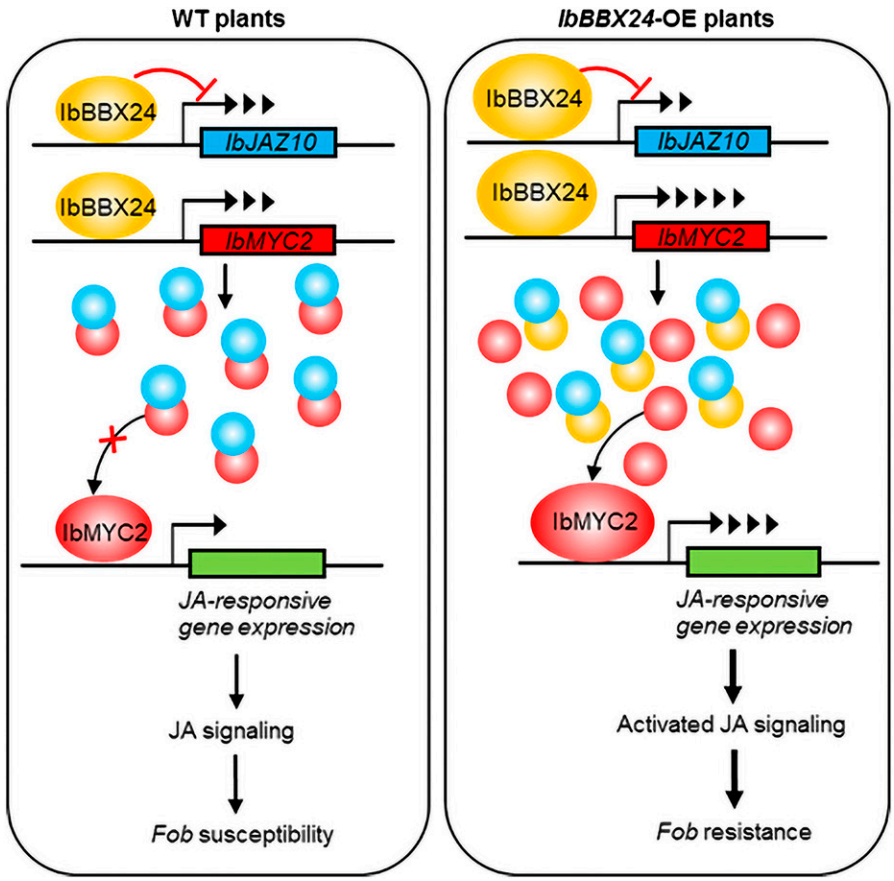

Figure 9. Proposed Working Model of the Role of IbBBX24 in JA-mediated *Fob* Resistance.

IbBBX24 binds to the promoters of *IbJAZ10* and *IbMYC2*, repressing *IbJAZ10* transcription but activating *IbMYC2* transcription. In *IbBBX24-OE* plants, elevated levels of IbBBX24 compete with IbMYC2 to interact with IbJAZ10 and enhance the ability of IbMYC2 to regulate its target genes. This process results in the activation of JA signaling, leading to *Fob* resistance. Yellow balls represent IbBBX24, blue balls represent IbJAZ10, and red balls represent IbMYC2. WT, wild type.

in Arabidopsis (Thatcher et al., 2009). However, different observations have been made regarding the infection mechanisms of various *F. oxysporum* f. sp in plants. For example, tomato *Fol* cannot secrete jasmonate-related metabolites, and the perturbation of JA signaling has no detectable effect on the susceptibility of tomato to *Fol* (Cole et al., 2014; Di et al., 2017). Consistent with these observations, we did not detect jasmonate-related metabolites (including JA, JA-Ile, and MeJA) in culture filtrates of *Fob* strains (Supplemental Table 4), indicating that jasmonate-related metabolites were not secreted by *Fob*. We conclude that *Fob* does not perturb the JA-signaling pathway in sweet potato by producing jasmonate-related metabolites, but additional studies are needed to further characterize its infection mechanisms. Nevertheless, our data demonstrate that IbBBX24 regulates *Fob* resistance in sweet potato by modulating both JA biosynthesis (Figure 2E) and JA signaling (Figure 9) in the host plant. Although we uncovered the molecular mechanisms underlying IbBBX24-mediated JA signaling, it would also be worth investigating how IbBBX24 regulates JA biosynthesis in sweet potato in the future.

The overexpression of *IbJAZ10* led to inhibited growth and decreased *Fob* resistance in tobacco (Figure 8). Consistent with these observations, the overexpression of JAZ proteins enhances susceptibility to pathogens and inhibits growth in several plant species (Chung and Howe, 2009; Yamada et al., 2012; de Torres Zabala et al., 2016; Ortigosa et al., 2019). Notably, the Arabidopsis activation-tagged line *jaz7-1D*, in which T-DNA was inserted in the *JAZ7* promoter to cause constitutive expression of this gene, displays increased susceptibility to *F. oxysporum* but enhanced JA-responsive gene expression (Thatcher et al. 2016). Perhaps the host JA-signaling pathway is hijacked by *F. oxysporum*, leading to hyperactive JA-signaling and senescence processes, and thus suppresses defense responses mediated by salicylic acid signaling (Thatcher et al. 2016).

Genetic immunity to disease is usually accompanied by unintended reductions in plant growth and yield (Ning et al., 2017). The yield penalties associated with disease resistance in crops was first reported for late blight disease in potato (*Solanum tuberosum*) in the early 1960s (Vanderplank, 1963). Since then, similar observations have been made in other crops (Jorgensen, 1992; Sharp et al., 2002; Ning et al., 2017). Thus, the balance between immunity and yield has become one of the most important issues in crop breeding (Ning et al., 2017). In this study, we showed that overexpressing *IbBBX24* significantly increased JA accumulation and signaling as well as *Fob* resistance in sweet potato. Moreover, overexpressing *IbBBX24* led to increased storage root yields (Supplemental Figures 5I and 5L). The molecular mechanism underlying IbBBX24-induced yield promotion in sweet potato is currently obscure. The formation and development of sweet potato storage roots is a complex process that is thought to be mediated by interactions of phytohormones such as auxins, GAs, and JAs (Ravi et al., 2009). Consistent with this notion, our ChIP-seq and RNA-seq data revealed a range of genes associated with auxins, GAs, and JAs (Supplemental Data Sets 2 and 3). Together, our study reveals *IbBBX24* as an ideal candidate gene for developing elite crop varieties with enhanced pathogen resistance but without yield penalty.

In summary, IbBBX24 plays a pivotal role in regulating the JA pathway, *Fob* resistance, and storage root yields in sweet potato. Because our current understanding of the interactions between JA signaling and *F. oxysporum* mainly comes from studies in Arabidopsis and tomato, and different infection mechanisms for invading plants may be adopted by different *F. oxysporum* f. sp, our study provides insights into the roles of JAs in regulating plant defense responses and developmental processes in crops.

METHODS

Plant Material and Growth Conditions

The *Fob*-resistant sweet potato (*Ipomoea batatas*) line ND98, *Fob*-susceptible variety Lizixiang, and tobacco (*Nicotiana tabacum*) cv W38 were used as the wild types. In vitro-grown transgenic sweet potato, ND98, and Lizixiang plants were cultured on Murashige and Skoog (MS) medium, and transgenic and W38 tobacco plants were cultured on half-strength MS medium at 27 ± 1°C under 13 h of cool-white fluorescent light at 54 μmol m^{-2} s^{-1}. The sweet potato plants were cultivated in the field, greenhouse, or growth chamber at the campus of China Agricultural University, Beijing, China.

Gene Identification and Phylogenetic Analysis

Total RNA was extracted using TRIzol Reagent (Invitrogen) from fresh leaves of *Fob*-susceptible Lizixiang and *Fob*-resistant ND98 plants at 0, 1, 2, and 3 d after inoculation with *Fob*. The corresponding cDNA was used for cDNA-AFLP analysis according to Leymarie et al. (2007). Fragments were separated on a sequencing polyacrylamide gel and visualized by silver staining according to Bassam et al. (1991).

The *IbBBX24* gene was cloned from *Fob*-resistant sweet potato line ND98 using rapid amplification of cDNA end. The ORF of *IbBBX24* was predicted using the ORF Finder (https://www.ncbi.nlm.nih.gov/orffinder/). Phylogenetic analysis of the deduced amino acid sequences of IbBBX24 and BBX proteins from Arabidopsis (https://www.arabidopsis.org/) was performed using the neighbor-joining method in MEGA6.0 with 1,000 bootstrap iterations (Figure 1C; Tamura et al., 2011). Multiple sequence alignment of the deduced amino acid sequences of IbBBX24 and other plant BBX proteins was conducted using the software DNAMAN (Lynnon-BioSoft). The alignments are shown in Supplemental File 1.

Isolation and Sequence Analysis of *IbBBX24*

Total RNA (TRIzol Reagent; Invitrogen) and genomic DNA (EasyPure Plant Genomic DNA Kit; TransGen) were extracted from fresh leaves of *Fob*-resistant ND98 plants. The corresponding cDNA fragments and genomic DNA sequences were amplified using *IbBBX24* primers (Supplemental Data Set 1) and analyzed as described by Zhang et al. (2019).

Expression Analysis in Sweet Potato

The leaves of pot-grown *Fob*-susceptible Lizixiang and *Fob*-resistant ND98 plants were sampled at 0, 0.5, 1, 2, and 3 d after inoculation with *Fob* at a spore density of 1.5×10^7 mL^{-1}. Four-week–old in vitro-grown plants were submerged in half strength MS medium containing 100 μM of MeJA and sampled at 0, 0.5, 1, 3, 6, and 12 h after treatment. Total RNA was extracted from leaf, stem, petiole, and root tissues of 4-week–old in vitro-grown *Fob*-resistant ND98 plants and from the leaf, stem, petiole, storage root, and fibrous root tissues of 3-month–old field-grown *Fob*-resistant ND98 plants using the TRIzol method (Invitrogen). RT-qPCR was conducted using the SYBR detection protocol (TaKaRa) on a 7500 Real-Time

PCR system (Applied Biosystems). The reaction mixture was composed of first-strand cDNA, primer mix, and SYBR Green M Mix (TaKaRa; code RR420A) to a final volume of 20 μL. The specific primers used in the assay are listed in Supplemental Data Set 1. A 169-bp fragment of the sweet potato *β-actin* gene (GenBank AY905538) was amplified with specific primers and used as an internal control (Supplemental Data Set 1).

Immunoblot Analysis

Anti-IbBBX24 polyclonal antibodies were produced by Beijing Protein Innovation. Briefly, sequence-validated pET-28a-IbBBX24 vectors (Novagen; B*am*HI and *Eco*RI sites) were introduced into competent *Escherichia coli* strain Transetta (DE3) cells to produce recombinant 6His-IbBBX24. 6His-IbBBX24 proteins were purified and used as antigens to immunize rabbits for the production of polyclonal antiserum. Antigen affinity-purified anti-IbBBX24 antibodies were used for immunoblot analysis.

Total proteins were extracted from the leaves of transgenic and wild-type plants in extraction buffer (50 mM of Tris-HCl at pH 8.0, 150 mM of KCl, 1 mM of EDTA, 0.5% Triton X-100, 1 mM of DTT, 1 mM of PMSF, and a 1× protease inhibitor cocktail tablet; Roche). The protein extracts were mixed with SDS sample buffer and detected by immunoblotting using anti-IbBBX24 antibodies (1:2,000 [v/v]) and anti-HSP antibodies (1:2,000 [v/v], AbM51099-31-PU; Beijing Protein Innovation) as a control. Goat anti-rabbit IgG (H+L) antibodies (1:5,000 [v/v], cat. no. 65-6120, Invitrogen) and rabbit anti-mouse IgG (H+L; 1:20,000 [v/v], cat. no. 31450, SK2477281E, Invitrogen) antibodies were used as secondary antibodies.

Subcellular Localization of IbBBX24

The entire *IbBBX24* coding region without the stop codon was amplified and subcloned into the *Spe*I and *Asc*I sites of binary vector pMDC83 (Curtis and Grossniklaus, 2003) to produce the *IbBBX24*-GFP fusion construct driven by the cauliflower mosaic virus 35S promoter. The plasmids were transformed into *Agrobacterium tumefaciens* strain EHA105. The translational fusion construct and a nuclear-localization marker (NLS-RFP) were transiently expressed in *Nicotiana benthamiana* leaf epidermal cells via *A. tumefaciens* infiltration (Verweij et al., 2008). The fluorescence signal was observed under a confocal laser-scanning microscope (LSM710; Zeiss).

Production of Transgenic Sweet Potato Plants

The coding region of *IbBBX24* was amplified from *Fob*-resistant line ND98 using a pair of specific primers and inserted into pBI121 to replace the glucuronidase gene (Supplemental Data Set 1). The *35S-IbBBX24-NOS* expression cassette was excised from the pBI121-*IbBBX24* vector and ligated between the same cleavage sites in pCAMBIA3301 to generate the overexpression vector pC3301-121-*IbBBX24*. To construct the RNAi plasmid, the non-conserved sequence of *IbBBX24* was identified using the sequence search tool InterProScan (http://www.ebi.ac.uk/Tools/pfa/iprscan/), and the tool RNAi Target Sequence Selector (http://bioinfo.clontech.com/rnaidesigner/frontpage.jsp) was used to provide suggestions for designing siRNA for the non-conserved sequence. The unique 346-bp sequence of *IbBBX24* (the upstream primer is at the 363th nucleotide and the downstream primer is at the 3′-UTR of *IbBBX24*; Supplemental Data Set 1) was cloned into RNAi vector pFGC5941 (McGinnis et al., 2005; digested with *Xho*I/*Swa*I for the forward fragment and with *Bam*HI/*Xba*I for the converse fragment). The expression vector pFGC5941-*IbBBX24* is under the control of the cauliflower mosaic virus 35S promoter and an NOS terminator, and the RNAi construct specifically targets *IbBBX24* due to the specificity of the target sequence. The two recombinant plasmids for overexpression and RNAi were each transfected into *A. tumefaciens* strain EHA105. Transformation and plant regeneration were performed using embryogenic suspension cultures of the *Fob*-susceptible variety Lizixiang as previously described by Liu et al. (2001) and Zhang et al. (2019).

Putative transgenic sweet potato plants overexpressing *IbBBX24* were identified using histochemical GUS assays as previously described by Jefferson et al. (1987). Blue staining of the tissues indicates a positive reaction. PCR analysis of the GUS-positive plants was conducted using 35S forward and *IbBBX24*-specific reverse primers (Supplemental Data Set 1) as previously described by Zhang et al. (2019). To identify *IbBBX24-Ri* plants, genomic DNA was extracted from the leaves of plantlets regenerated from callus tissue, and PCR was conducted using primers designed to bind within the CHSA intron of pFGC5941 (Supplemental Data Set 1).

Fusarium Wilt Resistance Assay

Cultures of the fungal pathogen *Fob* were incubated in the dark at 28°C on PDA plates for 1 week before use. For the mycelial infection method, *Fob* mycelial discs (1 cm in diameter) were obtained from the 8-cm–diameter position of a PDA plate. Cuttings (~25 cm) were obtained from 6-week–old field-grown plants and established in a transplanting box. A 1-cm–long wound was made in the stem using a sterile blade, and a mycelial disc was placed over the wound using sterile cotton. For the negative control, a 1-cm–long wound was made in the stem using a sterile blade and covered with a sterile PDA disc using sterile cotton. The relative humidity was maintained at 99%. The number of diseased leaves and the length of the necrotic regions on wounded stems were recorded. Three biological replicates consisting of pools of six plants were used.

For the spore infection method, fungal cultures grown on PDA plates were homogenized, suspended in sterile water, and adjusted to a spore density of 1.5×10^7 mL^{-1}. Transgenic and wild-type sweet potato cuttings (12 cm, without roots) and 40-d–old transgenic and W38 tobacco cuttings (without roots) were dipped into the spore solution for 30 min and cultivated in sterilized sand moisturized with sterilized Hoagland solution. Sterile water without spores was used as a negative control. The plants were irrigated with 100 mL of sterile water or 0.5 mM of MeJA solution per pot once daily. The relative humidity was maintained at 99%. The number of diseased leaves and the length of the necrotic regions of wounded stems were recorded. Three biological replicates consisting of pools of six plants were used. Sweet potato stem samples were collected for histological examination as described by Chai et al. (2014). Sweet potato leaf samples at 3 DAI with *Fob* were plated with gold and observed under a model no. SU3500 scanning electron microscope (Hitachi).

MeJA Treatment of *Fob*

Cultures of the fungal pathogen *Fob* were incubated in the dark at 28°C on PDA plates for 1 week before use. *Fob* mycelial discs (1 cm in diameter) were obtained from the 8-cm diameter position on each plate and cultured on new PDA medium containing 0, 0.1, 0.2, 0.5, 1.0, 2.0, 5.0, and 10.0 mM of MeJA. The mycelia and spores were observed under a model no. Ti-U microscope (Nikon) after 8 d of growth.

Transcriptome Analysis

Total RNA samples were extracted from the leaves of wild-type, *IbBBX24-OE* (OE-16), and *IbBBX24-Ri* (Ri-3) plants treated by the spore infection method at 1 DAI using the TRIzol method (Invitrogen). Two independent biological replicates were taken. The cDNA was sequenced using the HiSeq X Ten PE150 system (Illumina) according to the manufacturer's instructions. Clean reads for each sample were aligned to the reference genome of hexaploid sweet potato variety Taizhong 6 (https://www.ipomoea-genome.org/). The FDR was used to determine the threshold of

the P-value in multiple tests; a threshold of *FDR* < 0.05 determined by DESeq2 was considered to indicate differential expression.

Measurement of Pathogen Defense-related Indices

SOD activity, POD activity, H_2O_2 content, and MDA content (Zhang et al., 2019); total phenolic content (Velioglu et al., 1998); and lignin content (Syros et al., 2004) were measured as previously described. The JA contents of plants were quantified by indirect enzyme-linked immunosorbent assay as described in Yang et al (2001). The JA, JA-Ile, and MeJA contents in the culture filtrates of *Fob* strains were detected using the AB Sciex QTRAP 6500 liquid chromatography-tandem mass spectrometry platform according to the method of Cole et al. (2014).

ChIP Assay

The leaves of OE-16 plants infected with *Fob* at 1 DAI were used for the ChIP assay as described in Kaufmann et al. (2010). In brief, leaf tissue (~2 g) was cross-linked in 1% formaldehyde under a vacuum. The cross-linking was stopped by the addition of 0.125 M of Gly. The sample was ground to a powder in liquid nitrogen and subjected to nuclear isolation. Anti-IbBBX24 (1:150 dilutions) antibodies were used to immunoprecipitate the protein–DNA complex, and the precipitated DNA was recovered. The precipitated DNA (one biological replicate) was sequenced using the HiSeq 2500 SE50 system (Illumina) according to the manufacturer's instructions. Sequencing reads (100 bp) were mapped to the genome of hexaploid sweet potato variety Taizhong 6 using the software BWA v0.7.12 (Langmead et al., 2009; Yang et al., 2017). Model-based Analysis of ChIP-Seq v2.1.0 was used to implement a peak-finding algorithm to identify regions of IP enrichment against the background (Zhang et al., 2008). A Q-value threshold of enrichment of 0.05 was used for all data sets. The chromosome, peak width, fold enrichment, significance level, and peak summit number per peak distributions were all displayed.

Y1H Assay

For the Y1H assays, the coding sequences of genes were inserted into the pB42AD vector (Clontech), while the promoter fragments were cloned into the pLacZi2μ vector (Lin et al., 2007). All primers used to clone these constructs are listed in Supplemental Data Set 1. The vectors and the empty vector were transformed into yeast strain EGY48 by the PEG/LiAc method, and yeast cells were plated onto the first selective medium without Ura or Trp. Positive clones were cultured on the second selective medium (without Ura and Trp) containing Gal (20%), raffinose (20%), buffered salt (50 mL: 1.95 g of Na_2HPO_4 and 1.855 g of $NaH_2PO_4 \cdot 2H_2O$), and X-Gal for stringent screening of possible interactions according to the protocol of the Matchmaker One-Hybrid System (Clontech).

Dual-Luciferase Assay

The coding sequences of genes were cloned into the pGreenII 62-SK vector, which was used as an effector. The empty vector was used as a negative control. Promoter sequences were inserted into the pGreenII 0800-LUC vector, which was used as a reporter. The primers are listed in Supplemental Data Set 1. Protoplasts from sweet potato petioles were isolated and used for the dual-luciferase assays as previously described by Huang et al. (2018). Firefly LUC and *Renilla* luciferase (REN) activity levels were measured using the Dual-Luciferase Reporter Assay System (Promega). The LUC activity was normalized to REN activity. Three biological replicates were performed for this analysis.

EMSA

The sequence-validated pET-28a-*IbBBX24*, pET-28a-*IbMYC2*, and pET-28a-*IbJAZ10* vectors (*Bam*HI and *Eco*RI sites) were introduced into competent *E. coli* strain Transetta (DE3) cells to produce recombinant 6His-IbBBX24, 6His-IbMYC2, and 6His-IbJAZ10 proteins, respectively. The recombinant proteins were purified as previously described by Sun et al. (2017). The oligonucleotide probes for EMSAs were synthesized by Invitrogen. Labeled probes with biotin at the 5′ end were used as binding probes, whereas unlabeled probes were used as competitors. The primer and probe sequences are shown in Supplemental Data Set 1.

EMSAs were performed using a LightShift Chemiluminescent EMSA Kit (Thermo Fisher Scientific) according to the manufacturer's instructions. In brief, 20 nM of biotin-labeled probes were incubated with fusion proteins (1 μg) in binding buffer (20 mM of $MgCl_2$, 5% glycerol, 0.1% NP-40, and 0.1 mg mL^{-1} poly [dI-dC]). For the competition reaction, 2 mM (100×) unlabeled probes were mixed with the labeled probes. The DNA–protein complex was separated by electrophoresis in a 6% (w/v) native polyacrylamide gel. After separation, the biotin signal was detected using a Chemiluminescent Nucleic Acid Detection Module (Thermo Fisher Scientific) according to the manufacturer's protocol.

Protein Interaction Assay

The Y2H assay was performed as described in the Yeast Protocols Handbook (Clontech). The full-length (BD-IbBBX24) coding region and sequences encoding 98 amino acid residues at the N terminus (BD-IbBBX24^{N98}) and 133 amino acid residues at the C terminus (BD-IbBBX24^{C133}) of IbBBX24 were fused in-frame to the GAL4 DNA binding domain (GAL4 BD) in the *Bam*HI and *Eco*RI sites of the pGBKT7 vector (Invitrogen). BD-IbBBX24^{N98} was used as bait for Y2H screening. The cDNA in the pGADT7 plasmid library was fused to the GAL4 activation domain (GAL4 AD). These constructs were transformed into yeast strain Y2H Gold using the lithium acetate method. The yeast cells were plated onto synthetic defined (SD) medium lacking Ade/His/Leu/Trp (SD/−Ade/−His/−Leu/−Trp) and containing 3 mM of 3-aminotriazole (3AT) for stringent screening of possible interactions.

For the BiFC assay, IbBBX29, which shares 15.74% amino acid sequence homology with IbBBX24, was used as a related non-interacting protein for the negative control. IbBBX24 and IbBBX29 were cloned into the pSPYNE-35S vector and fused to the N terminus of YFP, respectively, whereas IbJAZ10 was cloned into the pSPYCE-35S vector and fused to the C terminus of YFP (Walter et al., 2004). These vectors were transformed into *A. tumefaciens* strain EHA105 and coinjected into *N. benthamiana* leaves. After 48 h of growth, yellow fluorescent signals were observed under a confocal laser-scanning microscope (model no. LSM710; Zeiss) with an argon laser (488-nm excitation wavelength).

For the LCI assay, the full-length *IbBBX24* and *IbJAZ10* coding regions were fused with the N- and C-terminus–encoding regions of the luciferase reporter gene, respectively (Chen et al., 2008). *Agrobacterium* harboring the nLUC-IbBBX24 and IbJAZ10-cLUC constructs were coinfiltrated into *N. benthamiana*, and the infiltrated leaves were analyzed for LUC activity at 48 h after infiltration using chemiluminescence imaging.

For the co-IP assay, total protein samples extracted from *N. benthamiana* leaves were tagged with Myc and HA in co-IP buffer (50 mM of Tris-HCl at pH 8.0, 150 mM of KCl, 1 mM of EDTA, 0.5% Triton X-100, 1 mM of DTT, 1 mM of PMSF, and a 1× protease inhibitor cocktail tablet; Roche). The protein extracts were mixed with anti-HA agarose beads (A2095; Sigma-Aldrich) and incubated at 4°C for 2 h. After at least five washes, the agarose beads were recovered and mixed with SDS sample buffer. The samples were detected by immunoblotting using anti-Myc (M4439, 026M4825V; Sigma-Aldrich) and anti-HA (H3663, 066M4837V; Sigma-Aldrich) antibodies. Rabbit anti-mouse IgG (H+L; 1:20,000 [v/v], 31450, SK2477281E; Invitrogen) secondary antibodies were used as the secondary

antibodies. The primer sequences are shown in Supplemental Data Set 1. Three biological replicates from different plants were performed for this analysis.

Production of Transgenic Tobacco Plants

The coding region of *IbJAZ10* was amplified from *Fob*-resistant sweet potato line ND98 using a pair of specific primers and inserted into pBI121 to replace the *glucuronidase* gene (Supplemental Data Set 1). The *35S-IbJAZ10-NOS* expression cassette was excised from the pBI121-*IbJAZ10* vector and ligated between the same cleavage sites in pCAMBIA3301 to generate the overexpression vector pC3301-121-*IbJAZ10*. This recombinant plasmid was transferred into *N. tabacum* cv W38 via *A. tumefaciens*-mediated transformation as described in Horsch et al. (1985). The integration of the transgene into different transgenic lines was confirmed by GUS assay and PCR.

Statistical Analysis

All data were analyzed using one-way ANOVA, two-way ANOVA, or a two-tailed Student's *t* test with the software SPSS 25.0 (https://www.ibm.com/support/pages/downloading-ibm-spss-statistics-25; Supplemental File 2). The values are represented as the means ± SD.

Accession Numbers

Sequence data from this article can be found in the GenBank data library under accession numbers *IbBBX24* (MH813941), *IbJAZ10* (MH813942), and *IbMYC2* (MH813943) and the Sweetpotato Genome and Resource Database Entry (http://sweetpotato-garden.kazusa.or.jp/) under accession numbers *IbCHI* (ltr_sc000305.1_g00007.1), *IbNAC72* (ltr_sc000543.1_g00010.1), *IbCRK* (ltr_sc002362.1_g00002.1), and *IbCOI1* (ltr_sc000034.1_g00002.1). The RNA-seq data (Series GSE140181) and ChIP-Seq data (Series GSE140281) were deposited in Gene Expression Omnibus (Series GSE140283).

Supplemental Data

Supplemental Figure 1. Tissue-specific expression, sequence analysis, and subcellular localization of *IbBBX24*.

Supplemental Figure 2. Specificity of the anti-IbBBX24 polyclonal antibodies used for immunoblot and ChIP analyses.

Supplemental Figure 3. Production of *IbBBX24* transgenic sweet potato plants.

Supplemental Figure 4. The *IbBBX24*-homologous genes were not knocked down due to cross silencing of RNAi.

Supplemental Figure 5. Morphology of *IbBBX24* transgenic and wild-type plants.

Supplemental Figure 6. Mock treatments for the Fusarium wilt resistance assay.

Supplemental Figure 7. Statistical analysis of the disease phenotypes of *Fob*-resistant line ND98, wild-type, and *IbBBX24* transgenic plants.

Supplemental Figure 8. MeJA affects the growth and development of *Fob*.

Supplemental Figure 9. Mock treatments for the Fusarium wilt resistance assay with or without MeJA treatment.

Supplemental Figure 10. Heat map of DEGs in wild-type, *IbBBX24-OE*, and *IbBBX24-Ri* plants at 1 DAI with *Fob*.

Supplemental Figure 11. KEGG enrichment analysis based on RNA-Seq and ChIP-seq data.

Supplemental Figure 12. Heat maps of DEGs based on RNA-seq analysis of OE-16, Ri-3, and wild-type plants at 1 DAI with *Fob*.

Supplemental Figure 13. SOD activity, POD activity, H_2O_2 contents, MDA contents, total phenolic contents, and lignin contents of transgenic and wild-type plants at 0, 1, and 3 DAI by the spore infection method.

Supplemental Figure 14. IbBBX24 regulates *IbCHI* and *IbCRK* expression by binding directly to their promoters.

Supplemental Table 1. Thirty-two DEGs between *Fob*-resistant ND98 and *Fob*-susceptible Lizixiang, as detected by cDNA-AFLP analysis.

Supplemental Table 2. Mapping rates of RNA-seq reads aligned to different sweet potato reference genomes.

Supplemental Table 3. List of IbBBX24-interacting proteins, as identified by Y2H assays.

Supplemental Table 4. JA, JA-Ile, and MeJA contents in axenic *Fob* cultures.

Supplemental Data Set 1. Sequences of the primers used in this study.

Supplemental Data Set 2. DEGs identified by RNA-seq from OE-16, Ri-3, and wild-type plants at 1 DAI with *Fob*.

Supplemental Data Set 3. Candidate target genes of IbBBX24, as determined by ChIP-seq.

Supplemental Data Set 4. Overlapping targets of IbBBX24 identified by ChIP-seq and RNA-seq.

Supplemental File 1. Alignments used to create Figure 1C and Supplemental Figures 1C and 4A.

Supplemental File 2. ANOVA and *t* test tables.

ACKNOWLEDGMENTS

This work was supported by the National Natural Science Foundation of China(grant 31771856), the Beijing Food Crops Innovation Consortium Program (grant BAIC09-2019), the China Agriculture Research System (grants CARS-10 and Sweetpotato), and the China Postdoctoral Science Foundation (grant 2018M630227).

AUTHOR CONTRIBUTIONS

S.H., Q.L., and H. Zhang conceived and designed the research; H. Zhang, Q.Z., J.H., Z.W., and Z.R. performed the experiments; H. Zhang, H. Zhai, Y.X., and N.Z. analyzed the data; H. Zhang and S.H. wrote the article; Q.L., J.L., X.W., S.G., and L.Y. revised the article; all authors read and approved the final version of the article.

Received August 20, 2019; revised January 22, 2020; accepted January 31, 2020; published February 7, 2020.

REFERENCES

Abuqamar, S., Chai, M.F., Luo, H., Song, F., and Mengiste, T. (2008). Tomato protein kinase 1b mediates signaling of plant responses to necrotrophic fungi and insect herbivory. Plant Cell **20:** 1964–1983.

Apel, K., and Hirt, H. (2004). Reactive oxygen species: Metabolism, oxidative stress, and signal transduction. Annu. Rev. Plant Biol. **55:** 373–399.

Bai, S., Tao, R., Tang, Y., Yin, L., Ma, Y., Ni, J., Yan, X., Yang, Q., Wu, Z., Zeng, Y., and Teng, Y. (2019). BBX16, a B-box protein, positively regulates light-induced anthocyanin accumulation by activating *MYB10* in red pear. Plant Biotechnol. J. **17:** 1985–1997.

Bassam, B.J., Caetano-Anollés, G., and Gresshoff, P.M. (1991). Fast and sensitive silver staining of DNA in polyacrylamide gels. Anal. Biochem. **196:** 80–83.

Berrocal-Lobo, M., and Molina, A. (2004). Ethylene response factor 1 mediates Arabidopsis resistance to the soilborne fungus *Fusarium oxysporum*. Mol. Plant Microbe Interact. **17:** 763–770.

Boter, M., Ruíz-Rivero, O., Abdeen, A., and Prat, S. (2004). Conserved MYC transcription factors play a key role in jasmonate signaling both in tomato and Arabidopsis. Genes Dev. **18:** 1577–1591.

Brisson, L.F., Tenhaken, R., and Lamb, C. (1994). Function of oxidative cross-linking of cell wall structural proteins in plant disease resistance. Plant Cell **6:** 1703–1712.

Campos, M.L., Kang, J.H., and Howe, G.A. (2014). Jasmonate-triggered plant immunity. J. Chem. Ecol. **40:** 657–675.

Chai, G., Qi, G., Cao, Y., Wang, Z., Yu, L., Tang, X., Yu, Y., Wang, D., Kong, Y., and Zhou, G. (2014). Poplar PdC3H17 and PdC3H18 are direct targets of PdMYB3 and PdMYB21, and positively regulate secondary wall formation in Arabidopsis and poplar. New Phytol. **203:** 520–534.

Chen, H., Zou, Y., Shang, Y., Lin, H., Wang, Y., Cai, R., Tang, X., and Zhou, J.M. (2008). Firefly luciferase complementation imaging assay for protein-protein interactions in plants. Plant Physiol. **146:** 368–376.

Chini, A., Fonseca, S., Chico, J.M., Fernández-Calvo, P., and Solano, R. (2009). The ZIM domain mediates homo- and heteromeric interactions between Arabidopsis JAZ proteins. Plant J. **59:** 77–87.

Chini, A., Fonseca, S., Fernández, G., Adie, B., Chico, J.M., Lorenzo, O., García-Casado, G., López-Vidriero, I., Lozano, F.M., Ponce, M.R., Micol, J.L., and Solano, R. (2007). The JAZ family of repressors is the missing link in jasmonate signalling. Nature **448:** 666–671.

Chung, H.S., and Howe, G.A. (2009). A critical role for the TIFY motif in repression of jasmonate signaling by a stabilized splice variant of the JASMONATE ZIM-domain protein JAZ10 in Arabidopsis. Plant Cell **21:** 131–145.

Cole, S.J., Yoon, A.J., Faull, K.F., and Diener, A.C. (2014). Host perception of jasmonates promotes infection by *Fusarium oxysporum* formae speciales that produce isoleucine- and leucine-conjugated jasmonates. Mol. Plant Pathol. **15:** 589–600.

Crocco, C.D., and Botto, J.F. (2013). BBX proteins in green plants: Insights into their evolution, structure, feature and functional diversification. Gene **531:** 44–52.

Crocco, C.D., Holm, M., Yanovsky, M.J., and Botto, J.F. (2010). AtBBX21 and COP1 genetically interact in the regulation of shade avoidance. Plant J. **64:** 551–562.

Crocco, C.D., Locascio, A., Escudero, C.M., Alabadí, D., Blázquez, M.A., and Botto, J.F. (2015). The transcriptional regulator BBX24 impairs DELLA activity to promote shade avoidance in *Arabidopsis thaliana*. Nat. Commun. **6:** 6202.

Crocco, C.D., Ocampo, G.G., Ploschuk, E.L., Mantese, A., and Botto, J.F. (2018). Heterologous expression of *AtBBX21* enhances the rate of photosynthesis and alleviates photoinhibition in *Solanum tuberosum*. Plant Physiol. **177:** 369–380.

Cui, H., Wang, Y., Xue, L., Chu, J., Yan, C., Fu, J., Chen, M., Innes, R.W., and Zhou, J.M. (2010). *Pseudomonas syringae* effector protein AvrB perturbs Arabidopsis hormone signaling by activating MAP kinase 4. Cell Host Microbe **7:** 164–175.

Curtis, M.D., and Grossniklaus, U. (2003). A gateway cloning vector set for high-throughput functional analysis of genes in planta. Plant Physiol. **133:** 462–469.

Datta, S., Hettiarachchi, G.H.C.M., Deng, X.W., and Holm, M. (2006). Arabidopsis CONSTANS-LIKE3 is a positive regulator of red light signaling and root growth. Plant Cell **18:** 70–84.

Datta, S., Johansson, H., Hettiarachchi, C., Irigoyen, M.L., Desai, M., Rubio, V., and Holm, M. (2008). LZF1/SALT TOLERANCE HOMOLOG3, an Arabidopsis B-box protein involved in light-dependent development and gene expression, undergoes COP1-mediated ubiquitination. Plant Cell **20:** 2324–2338.

Demianski, A.J., Chung, K.M., and Kunkel, B.N. (2012). Analysis of Arabidopsis *JAZ* gene expression during *Pseudomonas syringae* pathogenesis. Mol. Plant Pathol. **13:** 46–57.

Denness, L., McKenna, J.F., Segonzac, C., Wormit, A., Madhou, P., Bennett, M., Mansfield, J., Zipfel, C., and Hamann, T. (2011). Cell wall damage-induced lignin biosynthesis is regulated by a reactive oxygen species- and jasmonic acid-dependent process in Arabidopsis. Plant Physiol. **156:** 1364–1374.

de Torres Zabala, M., Zhai, B., Jayaraman, S., Eleftheriadou, G., Winsbury, R., Yang, R., Truman, W., Tang, S., Smirnoff, N., and Grant, M. (2016). Novel JAZ co-operativity and unexpected JA dynamics underpin Arabidopsis defence responses to *Pseudomonas syringae* infection. New Phytol. **209:** 1120–1134.

Devoto, A., Nieto-Rostro, M., Xie, D., Ellis, C., Harmston, R., Patrick, E., Davis, J., Sherratt, L., Coleman, M., and Turner, J.G. (2002). COI1 links jasmonate signalling and fertility to the SCF ubiquitin-ligase complex in Arabidopsis. Plant J. **32:** 457–466.

Di, X., Gomila, J., and Takken, F.L.W. (2017). Involvement of salicylic acid, ethylene and jasmonic acid signalling pathways in the susceptibility of tomato to *Fusarium oxysporum*. Mol. Plant Pathol. **18:** 1024–1035.

Dombrecht, B., Xue, G.P., Sprague, S.J., Kirkegaard, J.A., Ross, J.J., Reid, J.B., Fitt, G.P., Sewelam, N., Schenk, P.M., Manners, J.M., and Kazan, K. (2007). MYC2 differentially modulates diverse jasmonate-dependent functions in Arabidopsis. Plant Cell **19:** 2225–2245.

Douchkov, D., et al. (2016). The barley (*Hordeum vulgare*) cellulose synthase-like D2 gene (*HvCslD2*) mediates penetration resistance to host-adapted and nonhost isolates of the powdery mildew fungus. New Phytol. **212:** 421–433.

Du, M., et al. (2017). MYC2 orchestrates a hierarchical transcriptional cascade that regulates jasmonate-mediated plant immunity in tomato. Plant Cell **29:** 1883–1906.

Ebrahim, S., Usha, K., and Singh, B. (2011). Pathogenesis-related (PR)-proteins: Chitinase and β-1, 3-glucanase in defense mechanism against malformation in mango (*Mangifera indica* L.). Sci. Hortic. (Amsterdam) **130:** 847–852.

Ellis, C., and Turner, J.G. (2001). The Arabidopsis mutant *cev1* has constitutively active jasmonate and ethylene signal pathways and enhanced resistance to pathogens. Plant Cell **13:** 1025–1033.

Epple, P., Apel, K., and Bohlmann, H. (1997). Overexpression of an endogenous thionin enhances resistance of Arabidopsis against *Fusarium oxysporum*. Plant Cell **9:** 509–520.

Fan, X.Y., Sun, Y., Cao, D.M., Bai, M.Y., Luo, X.M., Yang, H.J., Wei, C.Q., Zhu, S.W., Sun, Y., Chong, K., and Wang, Z.Y. (2012). BZS1, a B-box protein, promotes photomorphogenesis downstream of both brassinosteroid and light signaling pathways. Mol. Plant **5:** 591–600.

Feys, B., Benedetti, C.E., Penfold, C.N., and Turner, J.G. (1994). Arabidopsis mutants selected for resistance to the phytotoxin

coronatine are male sterile, insensitive to methyl jasmonate, and resistant to a bacterial pathogen. Plant Cell **6:** 751–759.

Gangappa, S.N., and Botto, J.F. (2014). The BBX family of plant transcription factors. Trends Plant Sci. **19:** 460–470.

Gfeller, A., Liechti, R., and Farmer, E.E. (2010). Arabidopsis jasmonate signaling pathway. Sci. Signal. **3:** cm4.

Gimenez-Ibanez, S., Boter, M., Fernández-Barbero, G., Chini, A., Rathjen, J.P., and Solano, R. (2014). The bacterial effector HopX1 targets JAZ transcriptional repressors to activate jasmonate signaling and promote infection in Arabidopsis. PLoS Biol. **12:** e1001792.

Goossens, J., Swinnen, G., Vanden Bossche, R., Pauwels, L., and Goossens, A. (2015). Change of a conserved amino acid in the MYC2 and MYC3 transcription factors leads to release of JAZ repression and increased activity. New Phytol. **206:** 1229–1237.

Hassidim, M., Harir, Y., Yakir, E., Kron, I., and Green, R.M. (2009). Over-expression of CONSTANS-LIKE 5 can induce flowering in short-day grown Arabidopsis. Planta **230:** 481–491.

Hirakawa, H., et al. (2015). Survey of genome sequences in a wild sweet potato, Ipomoea trifida (H. B. K.) G. Don. DNA Res. **22:** 171–179.

Horsch, R.B., Fry, J.E., Hoffmann, N.L., Eichholtz, D., Rogers, S.G., and Fraley, R.T. (1985). A simple and general method for transferring genes into plants. Science **227:** 1229–1231.

Hou, X., Lee, L.Y.C., Xia, K., Yan, Y., and Yu, H. (2010). DELLAs modulate jasmonate signaling via competitive binding to JAZs. Dev. Cell **19:** 884–894.

Hu, Q., et al. (2018). Laccase *GhLac1* modulates broad-spectrum biotic stress tolerance via manipulating phenylpropanoid pathway and jasmonic acid synthesis. Plant Physiol. **176:** 1808–1823.

Hu, Y., Jiang, Y., Han, X., Wang, H., Pan, J., and Yu, D. (2017). Jasmonate regulates leaf senescence and tolerance to cold stress: Crosstalk with other phytohormones. J. Exp. Bot. **68:** 1361–1369.

Huang, C., Sun, H., Xu, D., Chen, Q., Liang, Y., Wang, X., Xu, G., Tian, J., Wang, C., Li, D., Wu, L., and Yang, X., et al. (2018). *ZmCCT9* enhances maize adaptation to higher latitudes. Proc. Natl. Acad. Sci. USA **115:** E334–E341.

Jefferson, R.A., Kavanagh, T.A., and Bevan, M.W. (1987). GUS fusions: Beta-glucuronidase as a sensitive and versatile gene fusion marker in higher plants. EMBO J. **6:** 3901–3907.

Jiang, L., Wang, Y., Li, Q.F., Björn, L.O., He, J.X., and Li, S.S. (2012). Arabidopsis STO/BBX24 negatively regulates UV-B signaling by interacting with COP1 and repressing HY5 transcriptional activity. Cell Res. **22:** 1046–1057.

Jiang, S., Yao, J., Ma, K.W., Zhou, H., Song, J., He, S.Y., and Ma, W. (2013). Bacterial effector activates jasmonate signaling by directly targeting JAZ transcriptional repressors. PLoS Pathog. **9:** e1003715.

Jorgensen, J.H. (1992). Discovery, characterization and exploitation of Mlo powdery mildew resistance in barley. Euphytica **63:** 141–152.

Katsir, L., Schilmiller, A.L., Staswick, P.E., He, S.Y., and Howe, G.A. (2008). COI1 is a critical component of a receptor for jasmonate and the bacterial virulence factor coronatine. Proc. Natl. Acad. Sci. USA **105:** 7100–7105.

Kaufmann, K., Muiño, J.M., Østerås, M., Farinelli, L., Krajewski, P., and Angenent, G.C. (2010). Chromatin immunoprecipitation (ChIP) of plant transcription factors followed by sequencing (ChIP-SEQ) or hybridization to whole genome arrays (ChIP-CHIP). Nat. Protoc. **5:** 457–472.

Khanna, R., Kronmiller, B., Maszle, D.R., Coupland, G., Holm, M., Mizuno, T., and Wu, S.H. (2009). The Arabidopsis B-box zinc finger family. Plant Cell **21:** 3416–3420.

Kidd, B.N., Edgar, C.I., Kumar, K.K., Aitken, E.A., Schenk, P.M., Manners, J.M., and Kazan, K. (2009). The mediator complex subunit PFT1 is a key regulator of jasmonate-dependent defense in Arabidopsis. Plant Cell **21:** 2237–2252.

Kim, S.K., Yun, C.H., Lee, J.H., Jang, Y.H., Park, H.Y., and Kim, J.K. (2008). *OsCO3*, a *CONSTANS-LIKE* gene, controls flowering by negatively regulating the expression of *FT*-like genes under SD conditions in rice. Planta **228:** 355–365.

Kloek, A.P., Verbsky, M.L., Sharma, S.B., Schoelz, J.E., Vogel, J., Klessig, D.F., and Kunkel, B.N. (2001). Resistance to *Pseudomonas syringae* conferred by an *Arabidopsis thaliana* coronatine-insensitive (*coi1*) mutation occurs through two distinct mechanisms. Plant J. **26:** 509–522.

Król, P., Igielski, R., Pollmann, S., and Kępczyńska, E. (2015). Priming of seeds with methyl jasmonate induced resistance to hemi-biotroph *Fusarium oxysporum* f. sp. *lycopersici* in tomato via 12-oxo-phytodienoic acid, salicylic acid, and flavonol accumulation. J. Plant Physiol. **179:** 122–132.

Langmead, B., Trapnell, C., Pop, M., and Salzberg, S.L. (2009). Ultrafast and memory-efficient alignment of short DNA sequences to the human genome. Genome Biol. **10:** R25.

Laurie-Berry, N., Joardar, V., Street, I.H., and Kunkel, B.N. (2006). The *Arabidopsis thaliana* JASMONATE INSENSITIVE 1 gene is required for suppression of salicylic acid-dependent defenses during infection by *Pseudomonas syringae*. Mol. Plant Microbe Interact. **19:** 789–800.

Leymarie, J., Bruneaux, E., Gibot-Leclerc, S., and Corbineau, F. (2007). Identification of transcripts potentially involved in barley seed germination and dormancy using cDNA-AFLP. J. Exp. Bot. **58:** 425–437.

Li, F., Sun, J., Wang, D., Bai, S., Clarke, A.K., and Holm, M. (2014). The B-box family gene *STO* (*BBX24*) in *Arabidopsis thaliana* regulates flowering time in different pathways. PLoS One **9:** e87544.

Li, L., Zhao, Y., McCaig, B.C., Wingerd, B.A., Wang, J., Whalon, M.E., Pichersky, E., and Howe, G.A. (2004). The tomato homolog of CORONATINE-INSENSITIVE1 is required for the maternal control of seed maturation, jasmonate-signaled defense responses, and glandular trichome development. Plant Cell **16:** 126–143.

Li, Y., Wang, Y., Zhang, H., Zhang, Q., Zhai, H., Liu, Q., and He, S. (2017). The plasma membrane-localized sucrose transporter IbSWEET10 contributes to the resistance of sweet potato to *Fusarium oxysporum*. Front. Plant Sci. **8:** 197.

Lin, R., Ding, L., Casola, C., Ripoll, D.R., Feschotte, C., and Wang, H. (2007). Transposase-derived transcription factors regulate light signaling in Arabidopsis. Science **318:** 1302–1305.

Liu, Q. (2017). Improvement for agronomically important traits by gene engineering in sweetpotato. Breed. Sci. **67:** 15–26.

Liu, Q., Zhai, H., Wang, Y., and Zhang, D. (2001). Efficient plant regeneration from embryogenic suspension cultures of sweetpotato. In Vitro Cell. Dev. Biol. Plant **37:** 564–567.

Liu, Y., Xing, L., Li, J., and Dai, S. (2012). Rice B-box zinc finger protein OsBBX25 is involved in the abiotic response. Zhiwu Xuebao **47:** 366–378.

Lorenzo, O., Chico, J.M., Sánchez-Serrano, J.J., and Solano, R. (2004). *JASMONATE-INSENSITIVE1* encodes a MYC transcription factor essential to discriminate between different jasmonate-regulated defense responses in Arabidopsis. Plant Cell **16:** 1938–1950.

Luo, X.M., et al. (2010). Integration of light- and brassinosteroid-signaling pathways by a GATA transcription factor in Arabidopsis. Dev. Cell **19:** 872–883.

McConn, M., Creelman, R.A., Bell, E., Mullet, J.E., and Browse, J. (1997). Jasmonate is essential for insect defense in Arabidopsis. Proc. Natl. Acad. Sci. USA **94:** 5473–5477.

McGinnis, K., Chandler, V., Cone, K., Kaeppler, H., Kaeppler, S., Kerschen, A., Pikaard, C., Richards, E., Sidorenko, L., Smith, T., Springer, N., and Wulan, T. (2005). Transgene-induced RNA interference as a tool for plant functional genomics. Methods Enzymol. **392:** 1–24.

McGrath, K.C., Dombrecht, B., Manners, J.M., Schenk, P.M., Edgar, C.I., Maclean, D.J., Scheible, W.R., Udvardi, M.K., and Kazan, K. (2005). Repressor- and activator-type ethylene response factors functioning in jasmonate signaling and disease resistance identified via a genome-wide screen of Arabidopsis transcription factor gene expression. Plant Physiol. **139:** 949–959.

Melotto, M., Mecey, C., Niu, Y., Chung, H.S., Katsir, L., Yao, J., Zeng, W., Thines, B., Staswick, P., Browse, J., Howe, G.A., and He, S.Y. (2008). A critical role of two positively charged amino acids in the Jas motif of Arabidopsis JAZ proteins in mediating coronatine- and jasmonoyl isoleucine-dependent interactions with the COI1 F-box protein. Plant J. **55:** 979–988.

Michielse, C.B., and Rep, M. (2009). Pathogen profile update: *Fusarium oxysporum*. Mol. Plant Pathol. **10:** 311–324.

Nagaoka, S., and Takano, T. (2003). Salt tolerance-related protein STO binds to a Myb transcription factor homologue and confers salt tolerance in Arabidopsis. J. Exp. Bot. **54:** 2231–2237.

Nepal, M.P., Andersen, E.J., Neupane, S., and Benson, B.V. (2017). Comparative genomics of non-tnl disease resistance genes from six plant species. Genes (Basel) **8:** 249.

Nicholson, R.L., and Hammerschmidt, R. (1992). Phenolic compounds and their role in disease resistance. Annu. Rev. Phytopathol. **30:** 369–389.

Ning, Y., Liu, W., and Wang, G.L. (2017). Balancing immunity and yield in crop plants. Trends Plant Sci. **22:** 1069–1079.

Ntui, V.O., Azadi, P., Thirukkumaran, G., Khan, R.S., Chin, D.P., Nakamura, I., and Mii, M. (2011). Increased resistance to Fusarium wilt in transgenic tobacco lines co-expressing chitinase and wasabi defensin genes. Plant Pathol. **60:** 221–231.

Ogawa, K., and Komada, H. (1985). Biological control of fusarium wilt of sweet potato with cross-protection by prior inoculation with nonpathogenic *Fusarium oxysporum*. Jpn. Agric. Res. Q. **19:** 20–25.

Ogawa, S., Kawahara-Miki, R., Miyamoto, K., Yamane, H., Nojiri, H., Tsujii, Y., and Okada, K. (2017). OsMYC2 mediates numerous defence-related transcriptional changes via jasmonic acid signalling in rice. Biochem. Biophys. Res. Commun. **486:** 796–803.

Oliveira, M.B., Junior, M.L., Grossi-de-Sá, M.F., and Petrofeza, S. (2015). Exogenous application of methyl jasmonate induces a defense response and resistance against *Sclerotinia sclerotiorum* in dry bean plants. J. Plant Physiol. **182:** 13–22.

Oliw, E.H., and Hamberg, M. (2017). An allene oxide and 12-oxophytodienoic acid are key intermediates in jasmonic acid biosynthesis by *Fusarium oxysporum*. J. Lipid Res. **58:** 1670–1680.

Ortigosa, A., Gimenez-Ibanez, S., Leonhardt, N., and Solano, R. (2019). Design of a bacterial speck resistant tomato by CRISPR/Cas9-mediated editing of *SlJAZ2*. Plant Biotechnol. J. **17:** 665–673.

Park, J.H., Halitschke, R., Kim, H.B., Baldwin, I.T., Feldmann, K.A., and Feyereisen, R. (2002). A knock-out mutation in allene oxide synthase results in male sterility and defective wound signal transduction in Arabidopsis due to a block in jasmonic acid biosynthesis. Plant J. **31:** 1–12.

Pauwels, L., et al. (2010). NINJA connects the co-repressor TOPLESS to jasmonate signalling. Nature **464:** 788–791.

Pauwels, L., and Goossens, A. (2011). The JAZ proteins: A crucial interface in the jasmonate signaling cascade. Plant Cell **23:** 3089–3100.

Pel, M.A., Foster, S.J., Park, T.H., Rietman, H., Arkel, G.V., Jones, J.D., Van Eck, H.J., Jacobsen, E., Visser, R.G.F., and Van der Vossen, E.A. (2009). Mapping and cloning of late blight resistance genes from *Solanum venturii* using an interspecific candidate gene approach. Mol. Plant Microbe **22:** 601–615.

Ping, Q., Cheng, P., Huang, F., Ren, L., Cheng, H., Guan, Z., Fang, W., Chen, S., Chen, F., and Jiang, J. (2019). The heterologous expression in *Arabidopsis thaliana* of a chrysanthemum gene encoding the BBX family transcription factor CmBBX13 delays flowering. Plant Physiol. Biochem. **144:** 480–487.

Qi, T., Song, S., Ren, Q., Wu, D., Huang, H., Chen, Y., Fan, M., Peng, W., Ren, C., and Xie, D. (2011). The Jasmonate–ZIM domain proteins interact with the WD-Repeat/bHLH/MYB complexes to regulate Jasmonate-mediated anthocyanin accumulation and trichome initiation in *Arabidopsis thaliana*. Plant Cell **23:** 1795–1814.

Qi, T., Wang, J., Huang, H., Liu, B., Gao, H., Liu, Y., Song, S., and Xie, D. (2015). Regulation of jasmonate-induced leaf senescence by antagonism between bHLH subgroup IIIe and IIId factors in Arabidopsis. Plant Cell **27:** 1634–1649.

Ravi, V., Naskar, S.K., Makeshkumar, T., Babu, B., and Krishnan, B.P. (2009). Molecular physiology of storage root formation and development in sweet potato (*Ipomoea batatas* (L.) Lam.). J. Root Crops **35:** 1–27.

Ruan, J., Zhou, Y., Zhou, M., Yan, J., Khurshid, M., Weng, W., Cheng, J., and Zhang, K. (2019). Jasmonic acid signaling pathway in plants. Int. J. Mol. Sci. **20:** 2479.

Schaller, F., Biesgen, C., Müssig, C., Altmann, T., and Weiler, E.W. (2000). 12-Oxophytodienoate reductase 3 (OPR3) is the isoenzyme involved in jasmonate biosynthesis. Planta **210:** 979–984.

Sharp, G.L., Martin, J.M., Lanning, S.P., Blake, N.K., Brey, C.W., Sivamani, E., Qu, R., and Talbert, L.E. (2002). Field evaluation of transgenic and classical sources of wheat streak mosaic virus resistance. Crop Sci. **42:** 105–110.

Sheard, L.B., et al. (2010). Jasmonate perception by inositol-phosphate-potentiated COI1-JAZ co-receptor. Nature **468:** 400–405.

Song, S., Qi, T., Huang, H., Ren, Q., Wu, D., Chang, C., Peng, W., Liu, Y., Peng, J., and Xie, D. (2011). The Jasmonate–ZIM domain proteins interact with the R2R3-MYB transcription factors MYB21 and MYB24 to affect Jasmonate-regulated stamen development in Arabidopsis. Plant Cell **23:** 1000–1013.

Stintzi, A., Weber, H., Reymond, P., Browse, J., and Farmer, E.E. (2001). Plant defense in the absence of jasmonic acid: The role of cyclopentenones. Proc. Natl. Acad. Sci. USA **98:** 12837–12842.

Sun, D., Lu, X., Hu, Y., Li, W., Hong, K., Mo, Y., Cahill, D., and Xie, J. (2013). Methyl jasmonate induced defense responses increase resistance to *Fusarium oxysporum* f. sp. *cubense* race 4 in banana. Sci. Hortic. (Amsterdam) **164:** 484–491.

Sun, W., Gao, D., Xiong, Y., Tang, X., Xiao, X., Wang, C., and Yu, S. (2017). Hairy Leaf 6, an AP2/ERF transcription factor, interacts with OsWOX3B and regulates trichome formation in rice. Mol. Plant **10:** 1417–1433.

Syros, T., Yupsanis, T., Zafiriadis, H., and Economou, A. (2004). Activity and isoforms of peroxidases, lignin and anatomy, during adventitious rooting in cuttings of *Ebenus cretica* L. J. Plant Physiol. **161:** 69–77.

Tamura, K., Peterson, D., Peterson, N., Stecher, G., Nei, M., and Kumar, S. (2011). MEGA5: Molecular evolutionary genetics analysis using maximum likelihood, evolutionary distance, and maximum parsimony methods. Mol. Biol. Evol. **28:** 2731–2739.

Thaler, J.S., Owen, B., and Higgins, V.J. (2004). The role of the jasmonate response in plant susceptibility to diverse pathogens with a range of lifestyles. Plant Physiol. **135:** 530–538.

Thatcher, L.F., Cevik, V., Grant, M., Zhai, B., Jones, J.D., Manners, J.M., and Kazan, K. (2016). Characterization of a *JAZ7* activation-tagged

Arabidopsis mutant with increased susceptibility to the fungal pathogen *Fusarium oxysporum*. J. Exp. Bot. **67:** 2367–2386.

Thatcher, L.F., Gardiner, D.M., Kazan, K., and Manners, J.M. (2012). A highly conserved effector in *Fusarium oxysporum* is required for full virulence on Arabidopsis. Mol. Plant Microbe Interact. **25:** 180–190.

Thatcher, L.F., Manners, J.M., and Kazan, K. (2009). *Fusarium oxysporum* hijacks COI1-mediated jasmonate signaling to promote disease development in Arabidopsis. Plant J. **58:** 927–939.

Thines, B., Katsir, L., Melotto, M., Niu, Y., Mandaokar, A., Liu, G., Nomura, K., He, S.Y., Howe, G.A., and Browse, J. (2007). JAZ repressor proteins are targets of the SCF^{COI1} complex during jasmonate signalling. Nature **448:** 661–665.

Turner, J.G., Ellis, C., and Devoto, A. (2002). The jasmonate signal pathway. Plant Cell **14** (Suppl): S153–S164.

Valverde, F., Mouradov, A., Soppe, W., Ravenscroft, D., Samach, A., and Coupland, G. (2004). Photoreceptor regulation of CONSTANS protein in photoperiodic flowering. Science **303:** 1003–1006.

Vanderplank, J.E. (1963). Plant Diseases: Epidemics and Control. (Dordrecht: Elsevier).

Van Hemelrijck, W., Wouters, P.F.W., Brouwer, M., Windelinckx, A., Goderis, I.J.W.M., De Bolle, M.F.C., Thomma, B.P.H.J., Cammue, B.P.A., and Delaure, S.L. (2006). The Arabidopsis defense response mutant *esa1* as a model to discover novel resistance traits against *Fusarium* diseases. Plant Sci. **171:** 585–595.

Velioglu, Y.S., Mazza, G., Gao, L., and Oomah, B.D. (1998). Antioxidant activity and total phenolics in selected fruits, vegetables, and grain products. J. Agric. Food Chem. **46:** 4113–4117.

Verweij, W., Spelt, C., Di Sansebastiano, G.P., Vermeer, J., Reale, L., Ferranti, F., Koes, R., and Quattrocchio, F. (2008). An H^+ P-ATPase on the tonoplast determines vacuolar pH and flower colour. Nat. Cell Biol. **10:** 1456–1462.

Walter, M., Chaban, C., Schütze, K., Batistic, O., Weckermann, K., Näke, C., Blazevic, D., Grefen, C., Schumacher, K., Oecking, C., Harter, K., and Kudla, J. (2004). Visualization of protein interactions in living plant cells using bimolecular fluorescence complementation. Plant J. **40:** 428–438.

Wang, H., Zhang, Z., Li, H., Zhao, X., Liu, X., Ortiz, M., Lin, C., and Liu, B. (2013a). CONSTANS-LIKE 7 regulates branching and shade avoidance response in Arabidopsis. J. Exp. Bot. **64:** 1017–1024.

Wang, Q., Tu, X., Zhang, J., Chen, X., and Rao, L. (2013b). Heat stress-induced *BBX18* negatively regulates the thermotolerance in Arabidopsis. Mol. Biol. Rep. **40:** 2679–2688.

Weller, J.L., Hecht, V., Vander Schoor, J.K., Davidson, S.E., and Ross, J.J. (2009). Light regulation of gibberellin biosynthesis in pea is mediated through the COP1/HY5 pathway. Plant Cell **21:** 800–813.

Wu, S., et al. (2018). Genome sequences of two diploid wild relatives of cultivated sweetpotato reveal targets for genetic improvement. Nat. Commun. **9:** 4580.

Xie, D.X., Feys, B.F., James, S., Nieto-Rostro, M., and Turner, J.G. (1998). COI1: An Arabidopsis gene required for jasmonate-regulated defense and fertility. Science **280:** 1091–1094.

Xiong, C., et al. (2019). A tomato B-box protein *SlBBX20* modulates carotenoid biosynthesis by directly activating *PHYTOENE SYNTHASE 1*, and is targeted for 26S proteasome-mediated degradation. New Phytol. **221:** 279–294.

Xu, D., Jiang, Y., Li, J., Holm, M., and Deng, X.W. (2018). The B-box domain protein BBX21 promotes photomorphogenesis. Plant Physiol. **176:** 2365–2375.

Xu, D., Jiang, Y., Li, J., Lin, F., Holm, M., and Deng, X.W. (2016). BBX21, an Arabidopsis B-box protein, directly activates HY5 and is targeted by COP1 for 26S proteasome-mediated degradation. Proc. Natl. Acad. Sci. USA **113:** 7655–7660.

Xu, L., Liu, F., Lechner, E., Genschik, P., Crosby, W.L., Ma, H., Peng, W., Huang, D., and Xie, D. (2002). The SCF(COI1) ubiquitin–ligase complexes are required for jasmonate response in Arabidopsis. Plant Cell **14:** 1919–1935.

Yamada, S., Kano, A., Tamaoki, D., Miyamoto, A., Shishido, H., Miyoshi, S., Taniguchi, S., Akimitsu, K., and Gomi, K. (2012). Involvement of OsJAZ8 in jasmonate-induced resistance to bacterial blight in rice. Plant Cell Physiol. **53:** 2060–2072.

Yan, C., and Xie, D. (2015). Jasmonate in plant defence: Sentinel or double agent? Plant Biotechnol. J. **13:** 1233–1240.

Yan, H., Marquardt, K., Indorf, M., Jutt, D., Kircher, S., Neuhaus, G., and Rodríguez-Franco, M. (2011). Nuclear localization and interaction with COP1 are required for STO/BBX24 function during photomorphogenesis. Plant Physiol. **156:** 1772–1782.

Yang, J., et al. (2017). Haplotype-resolved sweet potato genome traces back its hexaploidization history. Nat. Plants **3:** 696–703.

Yang, J., Duan, G., Li, C., Liu, L., Han, G., Zhang, Y., and Wang, C. (2019). The crosstalks between jasmonic acid and other plant hormone signaling highlight the involvement of jasmonic acid as a core component in plant response to biotic and abiotic stresses. Front. Plant Sci. **10:** 1349.

Yang, J., Zhang, J., Wang, Z., Zhu, Q., and Wang, W. (2001). Hormonal changes in the grains of rice subjected to water stress during grain filling. Plant Physiol. **127:** 315–323.

Yang, Y., Ma, C., Xu, Y., Wei, Q., Imtiaz, M., Lan, H., Gao, S., Cheng, L., Wang, M., Fei, Z., Hong, B., and Gao, J. (2014). A zinc finger protein regulates flowering time and abiotic stress tolerance in chrysanthemum by modulating gibberellin biosynthesis. Plant Cell **26:** 2038–2054.

Yun, D.J., D'Urzo, M.P., Abad, L., Takeda, S., Salzman, R., Chen, Z., Lee, H., Hasegawa, P.M., and Bressan, R.A. (1996). Novel osmotically induced antifungal chitinases and bacterial expression of an active recombinant isoform. Plant Physiol. **111:** 1219–1225.

Zhai, Q., Yan, C., Lin, L., Xie, D., and Li, C. (2017). 7-jasmonates. In Hormone Metabolism and Signaling in Plants, J. Li, C. Li, and and S.M. Smith, eds (London: Academic Press).

Zhai, Q., Zhang, X., Wu, F., Feng, H., Deng, L., Xu, L., Zhang, M., Wang, Q., and Li, C. (2015). Transcriptional mechanism of jasmonate receptor COI1-mediated delay of flowering time in Arabidopsis. Plant Cell **27:** 2814–2828.

Zhang, F., et al. (2015). Structural basis of JAZ repression of MYC transcription factors in jasmonate signalling. Nature **525:** 269–273.

Zhang, H., Gao, X., Zhi, Y., Li, X., Zhang, Q., Niu, J., Wang, J., Zhai, H., Zhao, N., Li, J., Liu, Q., and He, S. (2019). A non-tandem CCCH-type zinc-finger protein, IbC3H18, functions as a nuclear transcriptional activator and enhances abiotic stress tolerance in sweet potato. New Phytol. **223:** 1918–1936.

Zhang, H., Zhang, Q., Wang, Y., Li, Y., Zhai, H., Liu, Q., and He, S. (2017a). Characterization of salt tolerance and *Fusarium* wilt resistance of a sweetpotato mutant. J. Integr. Agric. **16:** 1946–1955.

Zhang, H., Zhang, Q., Zhai, H., Li, Y., Wang, X., Liu, Q., and He, S. (2017b). Transcript profile analysis reveals important roles of jasmonic acid signalling pathway in the response of sweet potato to salt stress. Sci. Rep. **7:** 40819.

Zhang, Y., Liu, T., Meyer, C.A., Eeckhoute, J., Johnson, D.S., Bernstein, B.E., Nusbaum, C., Myers, R.M., Brown, M., Li, W., and Liu, X.S. (2008). Model-based analysis of ChIP-Seq (MACS). Genome Biol. **9:** R137.

Zhu, W., Wei, W., Fu, Y., Cheng, J., Xie, J., Li, G., Yi, X., Kang, Z., Dickman, M.B., and Jiang, D. (2013). A secretory protein of necrotrophic fungus *Sclerotinia sclerotiorum* that suppresses host resistance. PLoS One **8:** e53901.